

## Article

# Minute-Scale Forecasting of Wind Power - Results from the collaborative workshop of IEA Wind Task 32 and 36

Ines Würth <sup>1\*</sup>, Laura Valldecabres <sup>2</sup>, Elliot Simon <sup>3</sup>, Corinna Möhrlen <sup>4</sup>, Bahri Uzunoğlu <sup>5</sup>, Ciaran Gilbert <sup>6</sup>, Gregor Giebel <sup>3</sup>, David Schlipf <sup>7</sup>, and Anton Kaifel <sup>8</sup>

<sup>1</sup> Stuttgart Wind Energy, University of Stuttgart, Allmandring 5b, 70569 Stuttgart, Germany; wuerth@ifb.uni-stuttgart.de

<sup>2</sup> ForWind - University of Oldenburg, Institute of Physics, Küpkersweg 70, 26129 Oldenburg, Germany; laura.valldecabres@forwind.de

<sup>3</sup> DTU Wind Energy (Risø Campus), Technical University of Denmark, Frederiksborgvej 399, 4000 Roskilde, Denmark; ellsim@dtu.dk, grgi@dtu.dk

<sup>4</sup> WEPROG, Eschenweg 8, 71155 Altdorf/Böblingen, Germany, Willemoesgade 15B, 5610 Assens, Denmark; com@weprog.com

<sup>5</sup> Dept. of Engineering Sciences, Division of Electricity, Uppsala University, The Ångström Laboratory, Box 534, 751 21 Uppsala, Sweden; Dept. of Mathematics, Florida State University, Tallahassee, FL, USA, 32310; bahriuzunoglu@computationalrenewables.com

<sup>6</sup> Department of Electronic and Electrical Engineering, University of Strathclyde, 204 George St, Glasgow G11XW, UK; ciaran.gilbert@strath.ac.uk

<sup>7</sup> Wind Energy Technology Institute, Hochschule Flensburg, Kanzleistraße 91–93, 24943 Flensburg, Germany; david.schlipf@hs-flensburg.de

<sup>8</sup> Zentrum für Sonnenenergie- und Wasserstoff-Forschung Baden-Württemberg, Meitnerstraße 1, 70563 Stuttgart, Germany; anton.kaifel@zsw-bw.de

\* Correspondence: wuerth@ifb.uni-stuttgart.de; Tel.: +49-711-685-68285

Academic Editor: Emanuele Ogliari, Sonia Leva

Version February 4, 2019 submitted to Energies

<sup>1</sup> **Abstract:** The demand for minute-scale forecasts of wind power is continuously increasing with the growing penetration of renewable energy into the power grid, as grid operators need to ensure grid stability in the presence of variable power generation. For this reason, IEA Wind Tasks 32 and 36 together organized a workshop on “Very Short-Term Forecasting of Wind Power” in 2018 to discuss different approaches for the implementation of minute-scale forecasts into the power industry. IEA Wind is an international platform for the research community and industry. Task 32 tries to identify and mitigate barriers to the use of lidars in wind energy applications, while IEA Wind Task 36 focuses on improving the value of wind energy forecasts to the wind energy industry. The workshop identified three applications that need minute-scale forecasts: (1) wind turbine and wind farm control, (2) grid power balancing, (3) energy trading and ancillary services. The forecasting horizons for these applications range from around 1 s for turbine control to 60 minutes for energy market and grid control applications. The methods that can be applied to generate minute-scale forecasts rely on upstream data from remote sensing devices such as scanning lidars or radars, or are based on point measurements from met masts, turbines or profiling remote sensing devices. Upstream data needs to be propagated with advection models and point measurements can either be used in statistical time series models or assimilated into physical models. All methods have advantages but also shortcomings. The workshop’s main conclusions were that there is a need for more research into new minute-scale forecasting techniques and that more efforts should be directed towards enhancing quality and reliability of the forecasts. On the long term, standards are required to support the adoption of these methods.

21    **Keywords:** wind energy; minute-scale forecasting; forecasting horizon; Doppler lidar; Doppler radar;  
22    numerical weather prediction models

---

23    **1. Introduction**

24    In the past years, minute-scale forecasting of wind power has become an important research  
25    topic in the wind energy community. Whereas traditional forecasting techniques provide a forecasting  
26    horizon in the hour or day range [1], new methods allow to predict the power output of wind turbines  
27    or wind farms on a minute scale. Due to the increasing penetration of renewable energy power systems  
28    into the grid, there is a demand for minute-scale wind power forecasts, as grid operators need to  
29    ensure grid stability in spite of the highly fluctuating power sources. The forecasts become even more  
30    important with increasing sizes of wind farms of several 100 MW and especially if those wind farms  
31    conglomerate geographically as it is the case for offshore sites. The objective of this paper is to provide  
32    a summary of the needs of minute-scale forecasting and an overview of the developed methods and  
33    the possible solutions to the barriers that prevent end users from adopting them.

34    The results presented in this paper are based on the outcome of the collaborative IEA Wind Task  
35    32 and 36 workshop “Very Short-Term Forecasting of Wind Power” held in Roskilde, Denmark in June  
36    2018. IEA Wind Task 32: “Wind Lidar Systems for Wind Energy Deployment” is an international open  
37    platform with the objective of bringing together experts from the academic and industrial communities  
38    to identify and mitigate barriers to the use of lidar for wind energy applications. IEA Wind Task 36:  
39    “Forecasting of Wind Power” is focused on improving the value of wind energy forecasts to the wind  
40    energy industry. During the workshop, 39 participants from academia, forecasting service providers,  
41    wind farm operators as well as the lidar and wind turbine manufacturers discussed the future needs of  
42    minute-scale forecasting, the advantages and barriers of different forecasting techniques and strategies  
43    for overcoming those barriers.

44    This paper is organized as follows. Section 2 discusses the need for minute-scale forecasting  
45    and explains target forecasting horizons for different applications. In Section 4, different forecasting  
46    techniques are described. To that end, first a review of state-of-the art forecasting techniques and the  
47    gap that needs to be closed with new methods in order to achieve minute-scale forecasts is given. Then  
48    different approaches to close the gap are discussed and for each method barriers and possible solutions  
49    are given. In Section 6 challenges for the implementation and commercialization of the new methods  
50    are discussed and the paper is finalized with conclusions in Section 7.

51    **2. Intra-hour variability of wind power generation**

52    In 2017 Denmark was the country with the highest wind power penetration rate (44% of the  
53    annual consumption of electricity), followed by Portugal (24%) and Ireland (24%). In the case of  
54    Denmark, the maximum hourly penetration rate was over 140%. With a total net installed capacity of  
55    169 GW, the power generation capacity of wind power in Europe increased by almost 300% in the last  
56    10 years [2]. Given the expected rising penetration levels of wind power and the increasing size of on-  
57    and especially offshore wind farms feeding power into the grid at a single point [3], it becomes crucial  
58    to have more precise forecasts of wind power generation with lead times of few minutes ahead and  
59    temporal resolutions of seconds or minutes.

60    When generating a forecast, one useful practice is to consider the power spectral density (PSD)  
61    of the measured physical process to understand which time frequencies contribute to the variance  
62    of the signal. Peaks in the spectra correspond to larger relative fluctuations which are traditionally  
63    more difficult to capture and predict. This type of analysis is demonstrated in Larsen et. al [4] using  
64    long-term site measurements from Høvsøre test station and Horns Rev offshore wind farm in Denmark.  
65    Boundary layer wind spectra were resolved across cycles ranging from 0.1 seconds (10 Hz) to 1 year.  
66    Figure 1 presents a main result of that work which compares full scale wind PSDs at 50 m height both

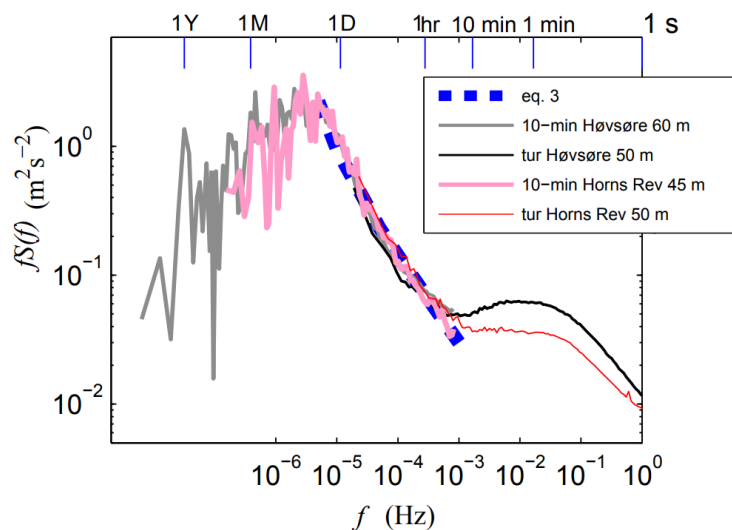


**Figure 1.** Power spectral density (PSD) of wind speed with corresponding timescales denoted atop. High frequency sonic measurements are used to devise the onshore (black) and offshore (red) lines. Reproduced with modifications from Larsen et. al [4] with permission from the Springer Nature publisher.

67 on- and offshore [4]. Apt [5] presents a similar PSD analysis of wind turbine output using 1-second  
 68 power data for a single wind turbine as well as a 6-turbine wind farm. Attributes of the PSD signal  
 69 will vary by location, time, sensor type, and physical property being measured. Still, from the results  
 70 in Figure 1, a strong local peak can be detected around 1 min, indicating the strong variability of the  
 71 wind at that temporal scale. This variability of the wind is associated to atmospheric phenomena like  
 72 open cellular convection, gravity waves, sea breezes or low level jets, among others [6]. At frequencies  
 73  $f > 0.02$  Hz, i.e. periods below one minute, the PSD signal strongly decreases and, as reported in [7],  
 74 wind power fluctuations of large wind farms are not considered an issue due to the smoothing effect  
 75 of aggregated power.

76 Yet, the intra-hour variability of wind power not only depends on the variability of the wind itself  
 77 but on the size of the wind farm, the number of wind turbines and their geographic dispersion. Indeed,  
 78 it has been shown by several authors that for offshore wind farms, the small geographic dispersion of  
 79 the wind turbines results in an increased power variability in the minute scale, compared to widely  
 80 dispersed onshore wind turbines [8].

81 The enhanced variability in those time scales leads to rapid changes in wind power generation  
 82 (ramp events). These unexpected events are mainly caused by extreme changes in wind speed and/or  
 83 direction in a very short period of time, and are frequently associated with the passage of weather  
 84 fronts. Despite being critical for the management of the grid, the dynamic allocation of reserves and the  
 85 stability of the system [9,10] there is no standard definition of a ramp event. Indeed, it is an individual  
 86 process of the end-user to define critical ramps and thereby ramp events. A recent publication on  
 87 the history of wind power ramp forecasting [11] gives an overview of the definitions used in ramp  
 88 event detection, the meteorological conditions associated to those events and the current forecasting  
 89 techniques. For most wind power forecasting applications however, the definition of what is critical for  
 90 an end-user is very individual and dependent on the application as well as the available reserves. For  
 91 example, a system operator on an island grid or badly interconnected grid needs to have all reserves  
 92 available within the control zone in order to prevent that a critical ramp could cause security issues. A  
 93 trader may also be very interested in ramp forecasts, as just one event with a large error may cause  
 94 95% of the imbalance costs in a month.

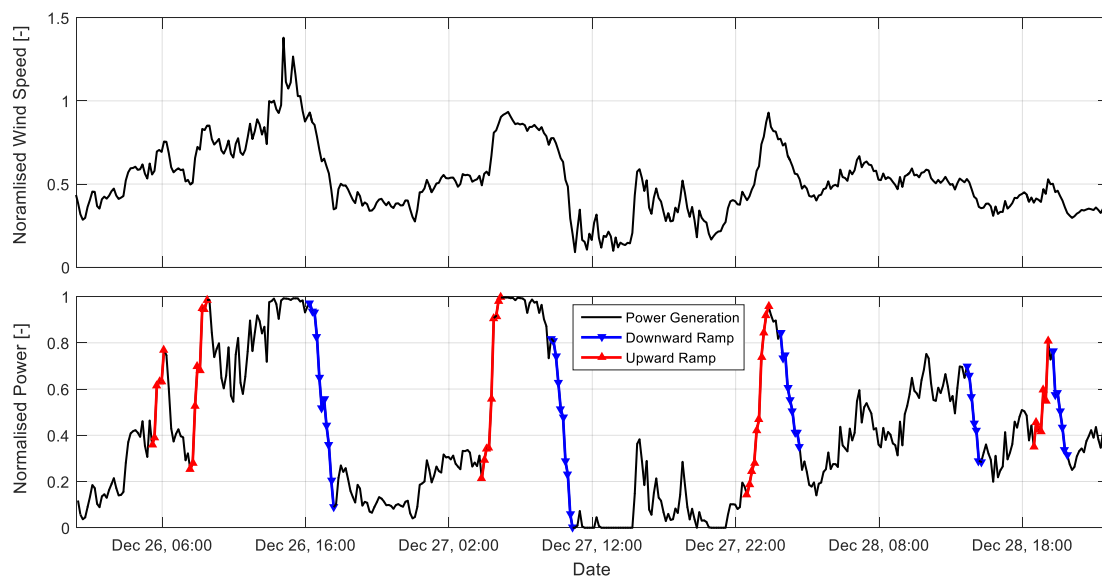


**Figure 2.** Example time series of wind speed and generated power of a single wind turbine with wind ramps marked for a time window of 60 min and a change of power of 40%. The time series is based on 10-minute averages. Reproduced without modifications from Würth et al. [12] with permission <https://creativecommons.org/licenses/by/3.0/>.

Ramp events are often classified into ramp-up and ramp-down events, according to the direction of the power gradient. As an example, the time-series in Figure 2 illustrates a number of steep ramps in both directions. While ramp-up events always can be handled in the very short term with curtailments, ramp-down events can become extremely critical due to the sudden missing generation. This enhances the importance of generating accurate minute-scale forecasts of wind power.

### 3. An overview of different applications for minute-scale forecasting in the wind industry

The forecast horizon and the parameters that are needed to be forecasted, depend on the application of the forecast. Three applications have been identified where minute-scale forecasts of wind speed or power are needed.

1. **Wind farm control:** Wind turbine and wind plant controllers need the information to optimize e.g. the power output of the turbines.
2. **Physical balancing:** They are required by the Transmission System Operator (TSO) in order to optimally operate reserves for the continuous balance of the power system and grid constraint management.
3. **Economic balancing:** Trading and balancing of wind power in the intra-day or rolling power markets require minute-scale updates of the forecasts with real power output in order to reduce imbalance costs and increase incomes.

It is expected that a next step in the evolution will be storage system planning and optimization in the real-time markets, where the bulk of the energy production will come from renewable energy sources. However, this paper focuses on the applications listed above. In the following each application is discussed in more detail.

#### 3.1. Wind turbine and wind farm control

Preview information of the wind field is helpful for the control of wind turbines and wind plants. Wind turbines are highly dynamic systems that are excited by stochastic influences from the

wind and most of the wind turbine control is designed to deal with variations in this disturbance. However, traditional feedback controllers are only able to react to impacts of wind changes on the turbine dynamics after these impacts have already occurred. Lidar-assisted control algorithms, which can exploit preview information of the wind, are promising to provide improved operation over conventional control algorithms, with the ultimate aim of increasing the energy yield while keeping the structural loads low. Regarding the required preview time, the following classification is useful:

1. around 1 s: Feedforward control is used to compensate wind changes to reduce structural loads. For e.g. the blade pitch, the rotor effective wind speed is needed only a short time before the wind reaches the rotor to overcome the pitch actuator dynamics.
2. around 5 s: For Model Predictive Control, the control inputs are optimized to get a chosen compromise of load reduction, energy production, and actuator wear [13]. Here, a short time horizon of wind characteristics such as wind speed, direction, and shear is used, typically 5-10 s.
3. around 1-10 min: For yaw control, a wind direction estimation is used to align the wind turbine with the mean wind direction. For this, a preview in the minute scale is helpful.

Active wind farm control is a promising technology to increase the energy production of wind farms [14]. However, flow models are still an important research topic, and the validation of flow models and control strategies is still ongoing. Wind preview for flow control is mainly used for induction control and wake steering for higher energy capture and management of fatigue loading. Regarding the required preview time, following classification is useful:

1. around 10 sec to 1 min for induction control: Usually the blade pitch angle is used to reduce the power and thrust to weaken wake effects on downstream turbines, which increase the overall production. At partial load this is done by adjusting the “fine pitch” settings which is usually based on a filtered wind speed estimate. Wind preview might help to better adjust the power balancing.
2. around 1-10 min for wake steering: The yaw misalignment is used to deflect wakes away from downstream turbines and thus similar preview times compared to the conventional yaw control is useful. A preview of the wind direction might help to better adjust the unintended yaw misalignments in a wind farm.

### 3.2. Power grid balancing, frequency control and power quality in reserve market

The focus in this section is on grid balancing, frequency control and power quality embedded in reserve market while the energy market and ancillary services are discussed in the following Section 3.3. The balancing term can be employed in a much broader sense in the context of balancing longer time scales. However in these time scales of mainly energy and reserve market, where balancing actions are scheduled before the real time, there are several other means of observations with lower resolutions available. [15–17]. However, these are not in the time scales of minute-scale forecasting that is the focus of this section. It should be noted that there are differences in terminology in different countries for same and slightly different balancing actions. In this section, the EU terminology is adopted for the rest of the discussions.

To guarantee the stability of the grid, supply and demand always have to be balanced in spite of the fluctuating power sources. Power quality is achieved if the grid frequency stays within a certain range of a rated value. An imbalance between supply and demand impacts voltage stability and grid frequency, hence there is a need for power balancing [15,18–20].

The volatility of wind resources creates volatility in the supply and as a result, balancing control actions are needed. One can distinguish between different time scales in this phase of controls embedded in the reserve market, which are known as primary, secondary, and tertiary control. The autonomous response of the system to supply/demand imbalances is automatically addressed with primary controls, which is in the scale of microseconds to seconds. In the secondary controls, there are automatic actions and manual actions in scales of seconds to minutes. In the tertiary controls, both

167 manual and automatic controls are in action from minutes to quarter of an hour to half an hour scale.  
168 All of these actions of balancing are carried out in order to ensure power system quality. Any forecast  
169 data that is available in scale of microseconds to minutes can be automatically employed in the state  
170 estimator of the controller [15,18–20]. The state estimator corrects with observational data, the state of  
171 the system.

172 From the market point of view, primary and/or secondary controls do not involve auction  
173 mechanisms. The participation to primary and secondary control can be traded by auction. This results  
174 in the availability of reserve for primary and/or secondary control. The market period can be day  
175 to year. The reserve market addressed in the context of primary and/or secondary controls consists  
176 of generators that can allocate themselves to be available as reserves for primary and/or secondary  
177 control. This availability is for a predefined time period for automatic control. This is achieved without  
178 any bidding as a result of commercial agreements or participation based on the context of the country.  
179 If there is utilization of reserve service, an utilization price is employed based on [21].

180 Wind power and other renewable energy create low levels of rotational inertia since these energy  
181 conversion systems do not normally act on rotational inertia which has impacts on the power grid  
182 frequency. Moreover asynchronous machines and Double Fed Induction Generator (DFIG) are  
183 disconnected by inverter from rotating mass of inertia. Suppliers have started to make changes  
184 to create synthetic inertia that can emulate inertia synthetically [22]. Synthetic inertia is about acting to  
185 AC frequency, possibly after the loss of a big power plant which makes the grid under-supplied and  
186 will result with the AC frequency beginning to fall. This makes the accurate short-term forecasting  
187 even more important since all of these emulations are dependent on accurate estimation of wind  
188 speeds. Hence automatic control for primary and/or secondary controls will certainly benefit from  
189 more accurate forecasting on the short-time scales of minutes in control applications.

### 190 3.3. Energy and ancillary services markets

191 Electricity markets need to be balanced in order to match the supply and demand of energy. This  
192 physical balancing of the transmission grid is carried out by the transmission system operators (TSO)  
193 or by an independent system operator (ISO). Given the increased integration of power generation from  
194 variable sources of energy like wind and solar, the physical balancing has become more complicated.  
195 Therefore, electricity markets with such intermittent and variable sources have to become more flexible  
196 and introduce either rolling markets (e.g. in the UK and Australia) or introduce shorter intra-day  
197 auctions, additional to the day-ahead auction, which have become very popular in Europe. Among  
198 the intra-day market platforms, one can distinguish between discrete auctions or continuous intra-day  
199 markets. In intra-day auction markets like in Italy, Spain or Portugal, intra-day bids are restricted  
200 to a few established auctions. By contrast, in continuous intra-day markets, counter parties match  
201 the bids using a trading platform that operates continuously. Those continuous intra-day balancing  
202 markets operate in Europe with different lead times ranging from 5 to over 100 minutes and most of  
203 the countries work with trading blocks of 15 minutes. Table 1 includes the lead times and smallest  
204 trading blocks for several countries in Europe and for Turkey. A more detailed description of the  
205 electricity markets and their time lines can be found in [23]. Hence, the importance of the use of  
206 updated available minute-scale forecast of wind power has arrived to stay.

**Table 1.** Lead times and smallest trading blocks for different countries. Sources: Epex [24], Nordpool [25], EXIST [26], and BSP South Pool [27].

Country	Lead time (minutes)	Trading blocks (minutes)	Market
Austria and Germany	5	15	EPEX Spot
Bulgaria, Denmark, Estonia, Finland, Lithuania, Norway and Sweden	60	15	NordPool
Belgium, France and the Netherlands	5	60	EPEX Spot
Slovenia	60	15	BSP Southpool
Switzerland	30	15	EPEX Spot
Turkey	90	60	EXIST

207 In light of this, the forecast process can be split into three components: (1) production of a smooth  
 208 day-ahead forecast tuned for economic adjustment via the intra-day market, (2) targeting intra-day  
 209 forecasts for the predictable part of the day-ahead forecast errors and (3) application of forecasts  
 210 on minute-scale to manage the wind after gate closure of the intra-day. The two first components  
 211 correspond to current practices in long-term and short-term processes with some enhancements. The  
 212 third component is a process running on minute-scale with 1 or 2 hour look ahead [e.g. 28].

213 Minute-scale forecasts are also necessary when applying to provide ancillary services, secondary  
 214 or tertiary reserve or balancing capacity for the pool of large utilities. For instance, a recent pilot project  
 215 in Germany allows wind power generators to participate in the reserve market by down-regulating  
 216 their production. The possible or available power produced by the wind farms needs to be calculated  
 217 in one-minute intervals. Furthermore, the standard deviation of the percentage error of the possible or  
 218 available wind farm power, during the pilot phase, should be less than 5% [29].

#### 219 4. State-of-the-art of wind power forecasting

220 State-of-the-art wind power forecasting methodologies utilise wind speeds from weather forecasts  
 221 and on-site real-time measurements to compute wind power.

222 Figure 3 shows qualitatively the forecast error levels of a day-ahead, hours-ahead and  
 223 minutes-ahead forecast compared to a persistence error, where the persistence forecast is the most  
 224 recent available measurement. The qualitative visualisation of the forecast errors in the different  
 225 time scales shall be seen in the light of their starting point and forecast error growth over time. For  
 226 example the day-ahead forecast has an almost linear error growth and is typically responsible for  
 227 approximately 1/3 of the forecast error [30]. The day-ahead forecast also starts with an inherent error  
 228 at forecast time zero due to a number of aspects. In [30] these are described as for example (i) the  
 229 initial weather conditions; (ii) sub grid scale weather activity; (iii) coordinate transformations; (iv) the  
 230 algorithm used to compute the wind power; (v) imperfection of turbines and measurement errors.  
 231 For Pahlow et al. [30] one question remained: which fraction of this background error is caused by  
 232 imperfect initial conditions of the weather forecast and which fraction is due to erroneous wind power  
 233 parameterizations. They extrapolated the linear forecast error growth from 9-45 hours down to the  
 234 0 hour forecast and thereby estimated the background mean absolute error (MAE) just under 4% of  
 235 installed capacity. Part of of that gap of approximately 4% error at initial time can be reduced by the  
 236 hours ahead forecast with knowledge about the real power production. Pahlow et al. [30] characterised  
 237 this inherent error at the initial time to a mix of unknown technical and non-technical constraints at  
 238 the forecast location. These can be wind farm specific constraints, such as unknown non-availability of  
 239 wind turbines, but also errors due to the computation of the wind power at the site. The hours-ahead  
 240 forecast are steeper in it's error growth than the day-ahead and reaches this level typically around  
 241 4-8 hours ahead in time. This time span is the typical temporal influence radius of a measurement  
 242 [30]. The minute-scale and persistence forecasts are both starting at the zero error in their initialisation.  
 243 This is what characterises this forecasting time scale, where the current state of the power plant is

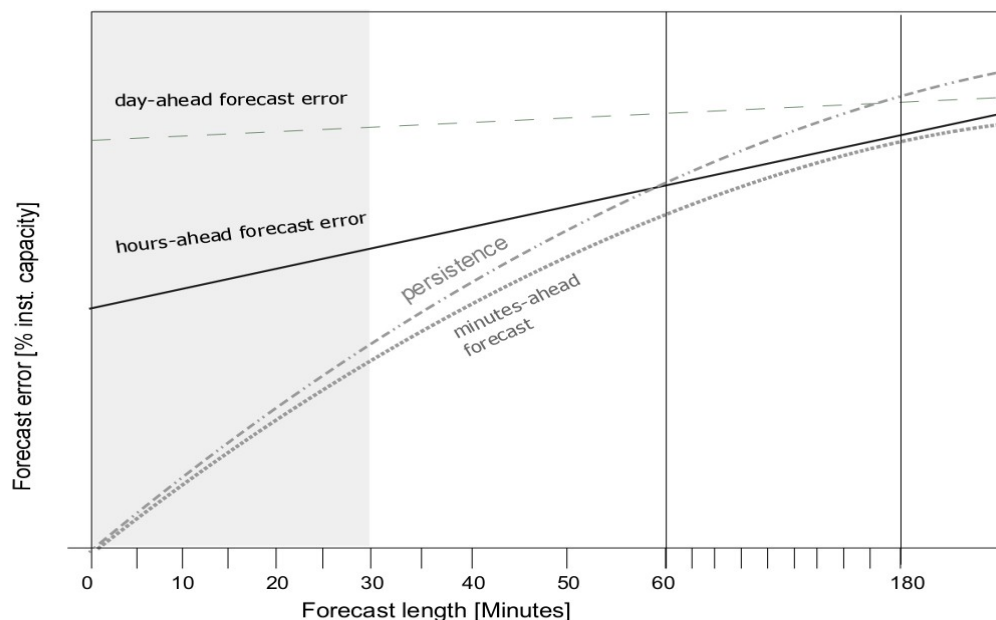


**Figure 3.** Qualitative visualisation of the forecast error development over the first hours of a forecast for different temporal forecast techniques.

fully known. The steepness of the error is also highest for these two forecast techniques due to the decrease of influence of the measurement at the power plant over time. A general industry experience is that a persistence forecast is at the same level as a hour-ahead forecast after around one hour. A minute-ahead forecast should ideally be below the hour-ahead forecast for about 3 hours as a thumb rule when evaluating the usefulness of the technique. The time between 1 hour and 3 hours into the forecast is where the persistence forecast typically reaches the day-ahead forecast error level and loses forecast skill.

Figure 3 illustrated nicely that the margin of possible improvements by minutes-ahead forecasts in the first 30 minutes of the forecast is rather small in comparison to persistence. Additionally, the average error growth of up to 2% of the installed capacity of a short-term forecast of 15 minute time resolution is rather steep (see Figure 3). It is therefore fair to say that the improvement over persistence, which is the objective in the very short time ranges of minutes and hours, is therefore rather modest. This is often used as a reason not to base decisions on forecasts, but rather use persistence, even during ramping, where the persistence forecast is a poor approximation. If the previous 15-minute forecast already appears to be off track, then the forecast user cannot justify to trust in the forecast. Also, the similarity between the average error of a short-term forecast and persistence over the next 15 minutes strongly indicates whether the short-term forecast has good or less good quality.

Forecast providers are continuously looking for enhancements, which can improve the hour-ahead and minute-scale forecast in the less good quality periods, because these result in the most significant power system benefits. Use of wind speed measurements in addition to wind power measurements is therefore a key to improve forecasts in periods, where the wind speed is in the flat ranges of the power curve ( $< 5 \text{ m/s}$  or  $> 12 \text{ m/s}$ ). Without wind speed measurements, the minute-scale forecast is in fact unable to correct the weather forecast for phase errors in periods, where the generation is zero or at full capacity.

A steady increase in wind speed from  $15 \text{ m/s}$  to above the high-speed shutdown point at  $25 \text{ m/s}$  can also be improved by using wind speed measurements in the short-term algorithms. At the high-speed shutdown points ( $> 25 \text{ m/s}$ ), the wind speed forecast uncertainty is at least  $2 \text{ m/s}$  even

271 in high predictability events. The timing of the shutdown is therefore uncertain, even a few minutes  
272 before it happens. Wind speed measurements from the wind farms reduce this uncertainty significantly.  
273 The timing of the high speed shutdown is important for grid security, because there are potentially  
274 many Megawatts instantly ramping down. In combination with forecasting on the minute-scale,  
275 such wind speed measurements can help to bridge the gap between the actual generation and both  
276 short-term and long-term forecast.

277 For wind speeds below the cut-in level there are similar considerations. Mostly, a cut-in wind  
278 speed occurs at a low aggregated wind power generation. Nevertheless, a large and strong low  
279 pressure centre may have near zero wind speeds from different directions. Both, the changes in  
280 wind direction and wind speed are better identified by wind speed measurements than wind power  
281 measurements. Thus, information about wind speeds below cut-in can be crucial for the forecast  
282 accuracy near a low pressure system centre at high aggregated wind power generation. During periods  
283 of moderate and high generation, wind speed measurements can be used to calculate current turbine  
284 availability or validate the delivered availability value. To conclude, measurements of low, medium  
285 and high wind speeds all add value to forecasting, while those measurement signals in the steep range  
286 of the power curve are least important.

287 From a technical perspective of the instrumentation, one of the most reported gaps for forecasting  
288 hours-ahead and minutes-ahead is the quality of the measurement signals. While wind farm developers  
289 have to use calibrated instrumentation and standardized methodologies in order to obtain a bankable  
290 level of siting accuracy in the first phase of a wind project, i.e. the planning and commissioning phase,  
291 the use of meteorological measurements is mostly not or badly defined, documented nor standardized  
292 in the following operational phase. Although the measurements are important in many ways, e.g.  
293 situational awareness in extreme events, scheduling and dispatch of generation on power system  
294 level, the balancing of large forecast errors, maintenance of instrumentation, there are no standards  
295 for the quality of the signals in real-time environments today. For example, if a measurement stops  
296 working correctly and sends constant values, a persistence forecast will benefit in a verification, while  
297 the forecast is penalized for providing a more realistic view of the situation. Dependent on the amount  
298 of such periods with constant values, this can easily lead to an overestimation of the performance of a  
299 persistence forecast in comparison to minutes-ahead forecasts and thereby prevent use and application  
300 of minutes-ahead forecasts.

301 Due to such missing standards and industry guidelines, the main gaps for the use of and collection  
302 of meteorological measurements and thereby advances in minute-scale forecasting can be summarized  
303 as:

- 304 • lack of requirements in the grid codes  
305 • lack of strategy for handling of missing or constant signals from measurements in real-time  
306 • lack of quality of measurements in real-time

## 307 5. Review of methods for minute-scale forecasting

308 In the previous section we discussed the state-of-the-art in minute-scale forecasting. In this section  
309 we investigate instrumentation that can improve forecasting with current techniques and we outline  
310 which and how new types of instrumentation can be used to improve forecasting on minute scale  
311 when persistence does no longer provide a correct picture of the weather conditions.

### 312 5.1. Minute-scale forecasting based on preview data from remote sensing devices

313 Remote sensing techniques are a new technology development in wind energy applications,  
314 which has its roots in the desire to find alternative measurements for expensive and at times difficult  
315 installation and erection of met masts.

316 With increasing experience and technical advances in technology, the remote sensing devices  
317 have become a real alternative. This has also been reflected in the IEC 61400-12-1 2017 standard [31],  
318 where such devices have been incorporated as possible instruments to carry out wind measurements

319 for wind energy applications. A new application for remote sensing devices is forecasting. Especially  
320 scanning devices such as scanning lidars and radars offer the possibility to carry out minute-scale  
321 forecasts by delivering high resolution temporal and spacial previews of the upstream wind field  
322 of a wind turbine or wind farm. Therefore, the next three sub sections give an overview of using  
323 those devices for forecasting purposes and finally lessons learned with remote sensing instruments in  
324 real-time forecasting projects are summarized.

325 5.1.1. Scanning lidar-based propagation models

326 Wind lidars can measure the line of sight (LOS) wind speed at distances from a few centimeters to  
327 several kilometers [32]. The first commercial wind lidar systems targeted at wind energy applications  
328 appeared in the early 2000's [33]. Because of their costs and ease of installation, lidars have become  
329 accepted as an alternative to the traditional mast-based wind sensors for site assessment and power  
330 performance testing, as evidenced by their inclusion in international standards [31]. Additionally,  
331 because they can measure upwind of operating turbines, wind lidars are used for feed-forward control  
332 of wind turbines [34]. For this application nacelle-based lidar systems are used to measure the wind  
333 speed several hundred meters upwind, thus forecasting the rotor effective wind speed seconds before  
334 it hits the rotor just in time to pitch the rotor blades and reduce loads. A new application for scanning  
335 lidars is wind power forecasting for power grid balancing. Commercial lidar manufacturers increased  
336 the range of their systems and pulsed compact scanning wind lidars may now measure up to 10 km  
337 away, enabling measurements across an entire site from one location [see e.g., 35,36]. There are also  
338 systems on the market that measure 30 km and more, but these systems have not been used for  
339 forecasting purposes. The basic idea is to use the spacial and temporal high resolution wind field  
340 information measured several kilometers upwind of a wind turbine or wind farm to forecast the power  
341 output ahead in time.

342 The forecast process (Figure 4) is the same for both applications – control and power grid  
343 balancing. First the raw lidar data is filtered for outliers and the horizontal wind speed and direction  
344 is reconstructed from the measured LOS wind speeds. Depending on the number of synchronized  
345 lidar measurements, different assumptions need to be made in order to resolve both horizontal wind  
346 speed and direction. For instance, a velocity-azimuth display (VAD) retrieval technique is used to  
347 resolve both wind speed and direction when only one lidar measurement is available [37]. This method  
348 assumes a homogeneous wind field and should only be used in flat terrain where the assumption  
349 is legit. Then the wind speed in the distance is propagated towards the wind turbine by means of a  
350 propagation model. The simplest model is based on Taylor's hypothesis which claims that turbulent  
351 eddies are transported with the mean flow and do not change their properties. With this assumption  
352 the time can be calculated that the wind speed measured in a certain distance needs to reach the turbine  
353 or wind farm. Thus the farthest measured distance determines the forecast horizon. The forecasted  
354 wind speed at the turbine or farm location is then used either to forecast the power output by means  
355 of a power curve or as an input to the wind turbine controller.

356 As mentioned, the forecast horizon is determined by the measurement distance of the lidar and  
357 the magnitude of the wind speed (Figure 5). For wind speeds at rated wind speed of a typical turbine,  
358 the maximum forecast horizon with a state-of-the-art long-range scanning lidar that ideally measures  
359 up to 10 km is around 15 min. The maximum horizon increases to around 40 minutes for a wind speed  
360 of 4 m/s that corresponds to a typical cut-in wind speed.

361 The advantage of scanning lidars is that they offer the possibility to directly measure the wind  
362 speed upstream of a turbine. All the long-range scanning lidars are pulsed devices, which means that  
363 the wind speed information is gathered simultaneously at different measurement distances. Thus the  
364 wind flow can be tracked over the span of the measurement and local changes in the wind speed are  
365 captured. Modern lidars have compact dimensions of around one cubic meter which allows for flexible  
366 measurement campaigns and the installation for instance on the nacelle of a wind turbine or other  
367 alleviated points such as an offshore substation. Then the scanning of the area on e.g. a horizontal arc

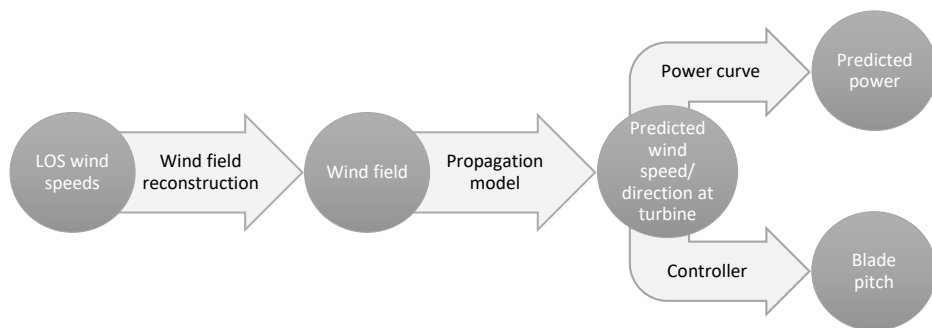


**Figure 4.** Forecast process using lidar data.

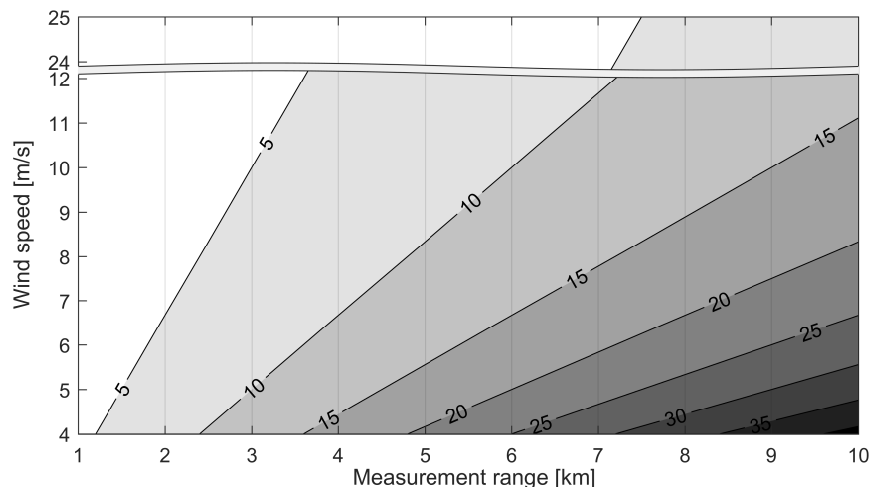


**Figure 5.** Forecast- horizon based on Taylor for different wind speeds and measurement ranges; horizon given in minutes.

368 leads to the desired horizontal wind speed information after reconstruction without having to take  
369 into account shear effects.

370 Recent investigations have shown that lidar-based forecasting models were able to predict  
371 near-coastal winds better than the benchmarks persistence and ARIMA for a forecasting horizon  
372 of 5 min [38]. Another relevant study is Simon et al. (2018) [39] which explores space-time correlations  
373 of upwind lidar observations measured on a flat horizontal plane. The study also shows results of a  
374 1-60 minutes ahead forecast method utilizing the lidar inflow scans which significantly outperforms  
375 the persistence method.

376 However, there are some drawbacks when using lidar data for forecasting. One of the major  
377 barriers to overcome is the availability of the measurements. The lidar measurement principle is  
378 based on the interaction of laser pulses with particles suspended in the air. The wavelength of the  
379 backscattered light is shifted relative to the speed of the aerosols according to the Doppler principle [40].  
380 This means that the measurement depends on the existence of these aerosols and if the concentration in  
381 the air is too high or too low, the device records a noisy signal. It also means that the measurement range  
382 fluctuates due to environmental conditions such as fog or rain showers [41]. And as the measurement  
383 range determines the forecast horizon, realtime forecasts are not possible if the lidar is blind. As  
384 physics cannot be changed, and the measurement principle is what it is, as a consequence a fallback  
385 solution needs to be implemented in case the lidar does not provide measurements. Data from other  
386 sensors such as radar or drone measurements could be one solution. Using statistical models (see  
387 Section 5.2) or the coupling of the measurements with NWP models (cf. Section 5.3) could be another  
388 solution. Also more investigations have to be carried out to determine the optimum conditions for  
389 good range measurements of lidars.

390 Another drawback of lidars so far have been the high costs and the inaccuracies of signals in  
391 complex terrain. According to the white paper of the Deutsche Windguard [42] and [43], especially  
392 "in complex terrain sites, influence of the relatively large scanning volume of today's LiDAR and  
393 SODAR must be carefully considered in terms of its influence on the measurement accuracy...". This  
394 has been a general observation and an ongoing research topic [see e.g., 44–49]. In one recent large  
395 scale measurement campaign, the Land-Atmosphere Feedback Experiment (LAFE), measurements  
396 were setup with multiple, synchronised scanning lidars that enable the direct measurements of  
397 wind field components [see e.g., 50,51]. Their instrument setup configuration addressed "the  
398 required combination of measurements for advanced studies of the land-atmosphere feedback" with a  
399 combination of instrumentation of scanning lidars and surface and airborne in situ measurements that  
400 provided the necessary overlap of measured data signals to fill gaps in the instrument's measurement  
401 ranges. This strategy could directly be transferred to the minute-scale forecasting problem in real-time  
402 environments and in complex terrain and is also widely applied in the data assimilation of NWP  
403 models (see section 5.3).

404 Another significant obstacle for the application of lidars in the wind power industry is the lack of  
405 standard or recommended practices for the use of scanning lidars for wind speed forecasting. More  
406 research is needed to find out what the ideal measurement setup looks like, in particular how many  
407 lidars are needed and where to place those devices within a wind farm or within a control zone of  
408 a system operator. Also, optimal measurement strategies need to be established and transferred to  
409 different problem areas and sizes. To that end different use cases have to be investigated to find out  
410 what the best campaign setup and measurement strategy is. Such use cases should include on- and  
411 offshore wind farms of different scales. Recommended practices then need to be consolidated so that  
412 the widespread use of lidar for forecasting becomes possible on a commercial level.

#### 413 5.1.2. Radar-based density models

414 Radars are remote sensing systems which can determine the position, angle or motion of objects  
415 and are being used in multiple applications including traffic control, ocean surveillance, weather  
416 monitoring, flight control systems and antimissile systems. Similar to wind lidars, Doppler radars

417 can be used for wind power forecasting as they are able to determine the velocity of the objects. The  
418 working principle is the same as for lidars, but rather than sending light waves, they emit radio waves.  
419 Thus, in an environment where meteorological particles with high humidity such as water droplets or  
420 ice crystals are present, radars are able to measure the wind speed by determining the motion of the  
421 hit particles.

422 The maximum range that radars can measure is given by the wavelength of the signal emitted, but  
423 in this paper we only focus on radars which work on wavelengths that are of interest for minute-scale  
424 forecasting of wind power. Thus, we limit our review to radars working between the C-Band and the  
425 Ka-band radars, or with a wavelength of 3.2 cm to 8.6 mm.

426 Doppler-radars working in the Ka-band (35 GHz) are optimal candidates for wind power  
427 forecasting (Figure 6). The short wavelength employed allows for high temporal and spatial resolution  
428 of the measured wind fields. As lidars, Doppler radars measure the LOS wind speed. Thus, measuring  
429 with one Doppler radar over a defined Plan Position Indicator (PPI) trajectory, the horizontal wind  
430 speed can be determined by applying a VAD retrieval technique. To derive the two horizontal wind  
431 speed components, two synchronized Doppler radars are needed [52]. The number of publications  
432 on the use of Doppler radars for wind energy applications has grown in the last years. Hirth et al.  
433 coupled wind farm operational data with wind fields measured by two synchronized Doppler radars  
434 (dual-Doppler radar) to further investigate wind farm wake effects [53]. Dual-Doppler measurements  
435 of the wake behind an offshore wind farm were also reported by Nygaard et al. [54]. The performance  
436 of wind turbines was also validated with dual-Doppler measurements in [55].

437 First evidence of the promising application of Doppler radar systems for forecasting purposes was  
438 documented by Hirth et al. [56]. An extreme wind ramp event observed by the Texas Tech University  
439 Ka-band radars at a wind farm in Oklahoma was presented. The authors merged dual-Doppler wind  
440 fields with operational data from 32 wind turbines to document the observed transient wind event  
441 and its effect on the wind turbines' performance. They also coupled data from a meteorological tower  
442 to analyze the weather conditions that originated the transient event.

443 Recently, it was shown that Doppler radar observations can be employed to derive minute-scale  
444 density forecasts of wind power. In [57] the authors proposed a methodology that uses dual-Doppler  
445 radar observations of wind speed and direction in front of a wind turbine to forecast the power  
446 generated in a probabilistic framework. In a case study, they predicted the power generated by seven  
447 turbines "free-wake" wind turbines in an offshore wind farm. Predictions were generated with a  
448 temporal resolution of one minute and with a lead time of five minutes. With their study, the authors  
449 showed that the radar-based forecasting model is able to outperform the persistence and climatology  
450 benchmarks in terms of overall forecasting skill and generate reliable density forecasts in the case of  
451 optimized trajectories.

452 One of the main advantages of Doppler radars is the extended range they can measure (over  
453 30 km). Additionally, the optimal trade-off between the temporal (one minute) and spatial (50 m)  
454 resolution of dual-Doppler radar measurements, compared to that of typical wind measurements from  
455 met-masts or satellites, makes them promising candidates for minute-scale forecasting of wind power.  
456 As with lidars, the same wind power forecasting process can be implemented to derive a wind power  
457 forecast. Besides, the fact that they can perform volumetric measurements (wind field measurements  
458 at multiple heights), allows to infer further information such as horizontal and vertical wind shear.

459 However, as with lidars, one of the main obstacles to the adoption of radar as a forecasting tool  
460 is the availability of the measurements. The radar measurement principle lies in the backscattering  
461 of particles in the air containing high humidity such as water droplets or ice crystals. Therefore, the  
462 quality of the measurements relies on the concentration of these particles in the air [52]. Besides, the  
463 relatively large dimensions of Doppler radars complicate their installation and reduces the range of  
464 possibilities for placing them, especially in offshore environments. The advantage of Doppler radar  
465 with respect to lidars is the maximum range that they can measure. However, compared to lidars, the  
466 wider beam width of radar results in larger beam spread at large ranges.



**Figure 6.** One of the two Doppler radar units deployed for the BEACON project [54,57].

#### 467 5.1.3. Weather radars for prediction of strong wind power fluctuations

468 Although we have mainly focused on the use of Doppler radars for forecasting applications,  
469 weather radars have been also identified as promising candidates for very short-term power forecasting  
470 of offshore wind power. Modern weather radars working in the C and X-band measure the intensity  
471 of precipitation. They are, consequently, able to anticipate precipitation fields associated with severe  
472 wind speed and power fluctuations. The capabilities of anticipating strong wind power fluctuations in  
473 offshore wind farms using local weather radars was introduced in [58,59]. In their work the authors  
474 were able to track the arrival of precipitation events to the surroundings of an offshore wind farm. These  
475 events were highly correlated with the strong observed power fluctuations. The authors also identified  
476 shortcomings of the use of weather radars for wind power forecasting, which included: interception of  
477 radar waves (cluttering), beam attenuation due to intense precipitation, anomalous propagation of  
478 the radar waves during specific atmospheric conditions, underestimation of precipitation reflectivity  
479 (beam filling) during convective events, and overshooting at long ranges due to the curvature of the  
480 Earth.

#### 481 5.1.4. Lessons learned with remote sensing instruments in real-time forecasting projects

482 Several research projects have been conducted with the goal of integrating remote sensing  
483 measurement into real-time forecasting projects. For this purpose not only scanning devices were  
484 deployed, but also profiling, ground-based devices. In the largest and longest measurement campaigns  
485 targeted towards real-time forecasting of wind energy in recent years were two projects funded by the  
486 United States Department of Energy, the wind forecasting improvement project (WFIP I and II) [60]  
487 there were used 12 wind profiling radars, 13 sodars and three lidars amongst other meteorological  
488 sensors. The lidars as well as sodars are basic equipment used in meteorological data assimilation  
489 today and have been quality checked following meteorological standards through the Meteorological  
490 Assimilation Data Ingest System (MADIS) [61]. This was a necessary step in order to improve the  
491 simulation into the real-time model forecast systems [62]. In the second project, "Distributed Resource  
492 Energy Analysis and Management System (DREAMS) Development for Real-time Grid", a number  
493 of sodars, lidars were used to enhance the Hawaiian system operator's EMS (Energy Management

494 System) tools for situational awareness in critical events [63]. Here, the instruments were for the first  
495 time part of the operational management system at a system operator in real-time.

496 From the above described studies and experimental measuring campaigns as well as real-time  
497 testing it can be concluded that the remote sensing instruments need to be serviced well and maintained  
498 similarly to any other real-time instrument operating under changing conditions throughout the yearly  
499 cycles. If this is not done, echoes, interfering noise sources, laser beam disturbances deteriorate  
500 the instruments and make the further processing of the data impossible and the quality of the data  
501 deteriorates significantly over time. It is also commonly understood that it requires skilled personnel  
502 to install and maintain such instrumentation, if it should run continuously and reliably.

503 The following lists their findings and recommended technical requirements to ensure high quality  
504 data in long-term real-time operation:

- 505 • Lightning protection and recovery strategy after lightning should be ensured.
- 506 • Instruments must be serviced and maintained by skilled staff.
- 507 • Version control must be maintained for signal processing.
- 508 • Measurements must be raw or technical requirements must include maintenance and software  
509 updates.
- 510 • Wind characteristics data should be measured at a height appropriate for the wind farm, either at  
511 hub height or preferable at both hub height and the lowest possible measuring height (e.g. 30 m).
- 512 • Remote sensing devices in complex terrain require special consideration.

513 From these findings and studied projects and measurement campaigns, it can be concluded that in  
514 active weather conditions, i.e. at the flat range of the power curve as well as under strong precipitation  
515 events, it must be expected that met mast anemometers are more reliable than sodar or lidar devices.  
516 From a forecasting and operational monitoring perspective, it has been found that the conditions  
517 outside of the instrument's range are some of the most critical conditions for grid operation, such as  
518 storms with precipitation or high winds. Sodars are more prone to data delivery failures than lidar,  
519 but to this date it is still also an issue for lidar devices that measurement information is not accessible  
520 in critical conditions, where it is most needed.

## 521 5.2. Statistical time series models

522 Statistical approaches to forecasting problems mainly rely on deducing patterns from past  
523 observational data and extrapolating these relationships to predict future values over a desired  
524 time step. With wind energy applications in mind, in this section we consider the task of forecasting  
525 a one dimensional time series signal such as a wind speed measurement, or a SCADA source such  
526 as wind turbine or wind farm active power signal. The chosen forecast horizon should relate to  
527 the time resolution of available input data, and at minimum be one sample (time step) ahead to  
528 avoid errors introduced by interpolation. Statistical forecasting methods used on the minute scale are  
529 largely identical to techniques employed for longer horizons. The main differences being the temporal  
530 resolution of the data and the variability of the physical process being predicted (see Section 2).

531 Data acquisition systems are ordinarily capable of sampling and saving data at high frequency,  
532 although historically this data has not always been used nor recorded. For the purposes of minute-scale  
533 forecasting, 10-minute or hourly averaged data sets are not sufficient for capturing signal characteristics  
534 needed to construct and validate a well performing statistical model. For this reason we recommend  
535 that all data generators ensure that they have access to and are logging their high frequency data (both  
536 turbine and meteorological sources), and that the instruments are properly maintained. The lower  
537 bound of the recorded sampling rate should be at minimum twice the highest frequency in the analog  
538 signal you wish to capture, in order to avoid aliasing in the discrete signal transformation (Nyquist  
539 sampling theorem). In practice, 1 Hz (1 sample per second) is proposed as a compromise between  
540 functionality and transmission/storage considerations. This will allow for future model building and  
541 testing which can resolve fluctuations on the minute-scale.

542 Time series data contrasts to cross-sectional data in that it is naturally ordered in time. Samples  
543 which are closer together will normally express a higher correlation than those further apart. This  
544 temporal link should be explored through inspection of the autocorrelation and partial autocorrelation  
545 function of the time series before beginning any attempts to build a model.

546 There are often a number of characteristic sub-components embedded in the time series which can  
547 be obtained through decomposition techniques in order to normalise samples across time. Examples  
548 include differencing an integrated series, removing an overall trend (usually by either mean subtraction  
549 or model fitting to obtain the residuals), accounting for cyclic fluctuations, and adjusting for seasonal  
550 variations.

551 A common assumption made by statistical forecasting methods is that of stationarity. Stationary  
552 processes comprise of data where the mean, variance, and autocorrelation structure do not change over  
553 time. By implementing the techniques described above, it is possible to transform a non-stationary  
554 time series into a stationary one which can be used with traditional forecasting methods.

555 Benchmarking in any forecasting exercise is crucial. Commonly for forecasting at these short  
556 timescales the persistence and climatology models are employed; these simple methods assume that  
557 the forecast for the target variable is the most recent available measurement or summary statistics of  
558 historical measurements, respectively. Statistical methods for wind speed and power forecasting are  
559 typically based on time-series models such as autoregressive [64] (AR) and autoregressive moving  
560 average (ARMA) [65,66] models as well as other soft computing techniques such as neural networks  
561 [67].

562 Purely AR models are formulated as a weighted combination of past observations (lags) where the  
563 coefficients are normally estimated via ordinary least squares regression. The order of the AR model,  
564 or maximum lag, is crucial and can be chosen most simply by inspection of the auto-correlation and  
565 partial auto-correlation functions of the signal. Cross-validation or an information criterion provide  
566 an alternative method for defining the model order. Domain knowledge of the local meteorological  
567 conditions can also be used to extend these simple models. For example, in certain regions the  
568 wind/power time series may exhibit strong diurnal trends which would necessitate the inclusion of  
569 time-of-day into the model.

570 Beyond time series models, machine learning techniques also are widely employed. These  
571 techniques can be more flexible than classic time series models in terms of easily allowing for more  
572 explanatory variables and are typically more naturally able to capture non-linear relationships. It  
573 should be noted that this comes at the expense of additional model tuning to optimize algorithm specific  
574 hyper-parameters and possible overfitting of the data unless careful cross-validation procedures are  
575 followed. Examples include artificial neural networks [67], hybrid multi-models with blending [68]  
576 together with feature selection [69], and penalized regression [70].

577 Artificial neural networks, particularly recurrent neural networks (RNN), have been widely  
578 applied for sequence prediction including time-series data. Long short-term memory (LSTM) networks  
579 are explicitly designed to capture data patterns of arbitrary lags, and assimilate long-term temporal  
580 dependencies [71]. This has led to numerous applications in energy forecasting which outperform  
581 traditional time-series modelling approaches. Wu et al. [72] demonstrates such a probabilistic 4-hour  
582 ahead wind power forecast model employing a LSTM network architecture.

583 Statistical forecasting models can also be made dependent on the current behaviour of the target  
584 time-series or on exogenous variable(s). These are termed regime-switching models and can be based  
585 on unobserved regimes [73,74] or by observed regimes like atmospheric conditions [75,76]. It follows  
586 that these regimes can be derived from lidar/radar measurements [59]. The benefit of regime switching  
587 is that the statistical models can react faster to changing conditions, as opposed to having a fixed  
588 coefficient models or by tracking slower changes in behaviour via for instance an online update of the  
589 coefficient estimates.

590 Concurrent information from spatially distributed wind farm or met mast measurements also  
591 provide a route for improvements in forecast skill [77,77]. Multivariate forecasts which encode

592 information on the spatio-temporal dependency of neighbouring sites can be tackled via a vector  
593 autoregressive models (VAR) at these time horizons. With an increasing number of sites, making  
594 sparse estimates of the coefficient matrices becomes more important, as does estimating them via  
595 efficient numerical procedures [78–80].

596 Forecast uncertainty at these horizons can also be accounted for via probabilistic density forecasts,  
597 quantiles, or prediction intervals [81]. These may be generated using parametric assumptions of the  
598 forecast distribution shape [64] [82] or non-parametric techniques [83] [84]. Uncertainty forecasts  
599 enable the user to manage risk in decision making and leverage more actionable information from  
600 their data, if information content is communicated properly [85].

601 These discussed statistical methods have been widely proven to increase forecast skill over  
602 persistence at time-horizons generally at a minimum of 10 minutes ahead. Further research is required  
603 to evaluate the suitability of statistical methods below this time horizon and at what time range  
604 forward facing lidar/radar based systems or hybrid statistical and radar/lidar systems are a more  
605 suitable choice.

### 606 5.3. Statistical data assimilation based on physical models

607 Data assimilation performs an essential role in the forecasts of wind power systems. While the  
608 concept is very inclusive, meaning inherently assimilation of any data with any model, in this section,  
609 the term is used in more exclusive sense without addressing statistical time series models, which is a  
610 special case of data assimilation where usually non-physical models are taken into consideration. This  
611 was discussed in the previous section. The concept is inherent from the fact that neither the model nor  
612 the observations are perfect. As a result to have an accurate state of the system, the numerical model  
613 without guidance of how accurate the current state is, is not sufficient and guidance from observations  
614 is required. This is even more so for weather forecast systems, where the system itself is very sensitive  
615 to initial conditions and boundary conditions. Data assimilation was employed first in engineering  
616 however it is more than an engineering tool today.

617 In summary, data assimilation is the technique to adopt multiple measurements and observations  
618 of different types into a 3-dimensional model space. In meteorology it is used to generate an initial  
619 state of the atmosphere from observations that is required as input field, together with boundary  
620 conditions to any numerical weather prediction (NWP) model.

621 In renewable energy production, data assimilation and state estimation also has an important  
622 role, in a classical way, but also with possibility of assimilation on control zone level or even park level.  
623 System operators and Wind farm operators require advanced knowledge of ramp-up and ramp-down  
624 events [86–88]. In a ramp/extreme event forecast you want to analyze and use outliers in order to get  
625 the risk of a critical ramp/event to occur, while some data assimilation algorithms can dismiss outliers.  
626 The increased frequency of assimilation can address this challenge. The frequency of assimilation  
627 is important for ramp prediction, while the challenge comes from the model size and assimilation  
628 method chosen for the task, however simplified models with higher frequency can be adapted for the  
629 applications discussed here.

630 The work on data assimilation and state estimation spans many disciplines and several decades in  
631 which many different methods have been developed to adapt the state of the atmosphere in numerical  
632 weather prediction models to large sets of measurements [89,90]. The initial development of data  
633 assimilation has started as an objective analysis [e.g., 91,92], which was also referred as successive  
634 correction methods.

635 This work was followed by optimum interpolation (OI) [e.g. 89,93]. Optimal Interpolation (OI)  
636 methods have lead to development of variational methods in data assimilation, where constraints  
637 were introduced in variational data assimilation methods. These methods are namely 1DVAR, 2DVAR,  
638 3DVAR [e.g. 94,95] and 4DVAR [96,97, e.g., ] where D stands for Dimension. Variational approaches  
639 can be also formulated in the context of a Bayesian problem.

In parallel sequential data assimilation techniques have been developed, where the model system is essentially corrected with observations rather than the model is fit to observations [e.g. 98,99]. The Kalman filter is a sequential data assimilation technique and was introduced as an observer feedback control system. The main difference between 4DVar and Kalman filters are the way that they address the mode and mean when the distributions are non-normal. There are several existing methods used in state estimation and data assimilation and most of them are based on the Kalman filtering theory introduced by Kalman and Bucy [100]. The pure form of the Kalman filter has been widely employed for the state estimation of the linear Gaussian systems [101], however it is linear and is not preferred for non-Gaussian and nonlinear systems [101,102]. For transition of Kalman filtering to the nonlinear and non-Gaussian systems, techniques such as extended Kalman filter (EKF), ensemble Kalman filter (EnKF), unscented Kalman filter (UKF) and particle filter (PF) algorithms are developed [101,102] and are employed to wide range of problems from low to high dimensional systems. The EKF method is implemented by linearisation of the non-linearities via using a Jacobian matrix. The EnKF uses Monte Carlo methods that helps to estimate the error covariances of the background error, gets an approximation to the Kalman-Bucy filter and produces an ensemble of initial conditions that can be utilized in an ensemble forecasting system. The EnKF embeds the non-linearities into the original linear KF solution and it uses an extra covariance inflation to consider the nonlinearities [98,103]. Later, adjustment solutions [e.g., 104] and also sequential solutions of the filter have been developed [e.g., 105].

Möhrlen et al. [28] found out that some of the limitation of the Kalman filter technique in meteorological context is however not a limitation in wind power context, because there the area of observational distribution is rather small, even if the area spans over an entire country. In atmospheric data assimilation the measurement data used is spread widely in space (globally), but is mostly sparse in time. In wind power context, observations are concentrated in small areas with high time resolution. A classical KF approach would not make sense as models would have to generate forecasts in a small area, which is undesired, or it would require unrealistically many computing resources and observational input of meteorological variables [28].

The classical Kalman Filter propagates the error covariances step-wise forward in time. This is computational expensive procedure [104,105]. To avoid the expensive computations this procedure can be approximated by using ensemble forecasts. This is the principle behind the ensemble Kalman Filter approaches.

The physical based ensemble prediction methods, especially the multi-scheme approach has been found as the most efficient method due to its ability to generate physically consistent spread in any time step with a much smaller ensemble size [106].

The unscented Kalman filter (UKF) employs the calculation of an approximate mean and covariance as a linear combination of a number of propagated points (called as sigma points). The PF and its variants also use the Monte Carlo simulation with sampling method based approximation of the posterior density of the state vector rather than doing any explicit functions so it simulates non-linearity and non-Gaussianity. Even though PF is a competent tool for the estimation of the nonlinear and non-Gaussian systems [107], it can be computationally demanding because of size that increases accuracy however this can be addressed adaptively with careful selection of ensembles introduced by Uzunoğlu [108].

The computational complexity in the above summarized methods can be addressed in the subspace of ensembles that was one of the focuses of the Maximum Likelihood Ensemble Filter (MLEF) that employs ensembles in the pre-conditioner. This approach differs from the EnKF and PF by working on state space rather than sample space and it optimizes a nonlinear cost function through maximum likelihood practice which reduces the computational time and addresses the stochasticity and the discontinuity while it utilizes the sampling in low dimensional space and employs the Hessian information. This method has been applied to many disciplines such as power systems as well as

689 to the wind energy industry [19,109]. In the workshop, the successful application of this method to  
690 second scales were presented.

691 *5.4. Extreme event forecasting models*

692 Extreme events in a meteorological sense are events that deviate from the mean and exceed  
693 beyond specific threshold values. In the power system, extreme events can occur under meteorological  
694 average conditions as well and not be considered extreme, when meteorological threshold values, such  
695 as wind speed, are exceeded. The differences are mainly due to the constraints in the power lines and  
696 the supply and demand relationship. Only in areas where wind turbines shut down due to high wind  
697 speeds - so called high-speed shutdowns can such wind speeds challenge both life and the ability to  
698 safely control the grid.

699 The way to deal with extreme events in both meteorology and the power industry is by applying  
700 uncertainty forecasts that provide an objective measure of the possible extreme. Deterministic forecasts  
701 cannot serve such situations, as they are tuned for best average conditions, i.e. in the setup, statistical  
702 training and model output statistics, outliers and extremes are filtered out. While statistical approaches  
703 can be used in many life science applications, in power system applications, it is crucial to employ  
704 an approach that provides a valid uncertainty of the forecast inclusive extremes in every hour of  
705 the forecast. Such extreme forecasts must be established based on probabilities computed from a  
706 probabilistic prediction system that can take the spatial and temporal scales into consideration in order  
707 to capture the temporal evolution and spatial scale of e.g. low pressure systems that contain wind  
708 speeds leading to large scale shut-down of wind farms.

709 This can for example be provided by such a physical approach based on a NWP ensemble that  
710 ideally contains all extreme values inherent in the approach without the requirement of statistical  
711 training such as the multi-scheme method. Alternative solutions may exist from statistical approaches  
712 by employing an extreme event analysis to a statistical ensemble [see e.g., 85]. However, statistical  
713 approaches are always limited to past climatology and require large amounts of data. The requirement  
714 for such forecasts is that they must be able to provide probabilities of extreme events, where each  
715 forecast or "forecast member" provides a valid and consistent scenario of the event. The probabilities  
716 need to be suitable solutions for a decision process. They can be computed for very critical and less  
717 critical events, depending on the end-users' requirements.

718 In meteorology the use of sophisticated observational instrumentation for data assimilation  
719 problems is an ongoing transformation throughout the last decades. As new technologies become  
720 available that in some way are able to reflect some part of the atmospheric system, where the model  
721 systems require parameterisations, such instrumentation is usually tested in research campaigns  
722 and then deployed at specific locations [see e.g., 106,110–113]. Transferring this knowledge to  
723 the assimilation of wind power observations that are irreversible in their nature is more complex.  
724 Nevertheless, a unified methodology that is able to decide on the value of an observational signal and  
725 its impact on the total system is required to solve this task.

726 In section 5.1.2 we learnt for example that radar measurements can be used for forecasting, but  
727 require transformation algorithms to be useful for the forward propagation of the data signals. The  
728 Kalman Filter techniques are practical approaches that have inherent capabilities to transform such  
729 data signals and use them in convective-scale data assimilation tasks (see e.g. [112,113]).

730 With ensemble Kalman Filter techniques, the input ensemble data can also be used to deal  
731 with the uncertainty of different types of measurements, also in the transformation phase of more  
732 advanced data signal technologies, if the signals are in relation with the target parameter [28]. The  
733 example in Figure 7 shows the functionality of an inverted Kalman Filter approach for the assimilation  
734 of point measurements in (wind and solar) power space with a multi-scheme ensemble approach  
735 described in [28]. In this schematic, power signals from wind and/or solar generating units and other  
736 related meteorological observation are assimilated with the help of a so-called multi-scheme ensemble,  
737 a physical based ensemble approach [28]. The ensemble contains 75 members with 13 different

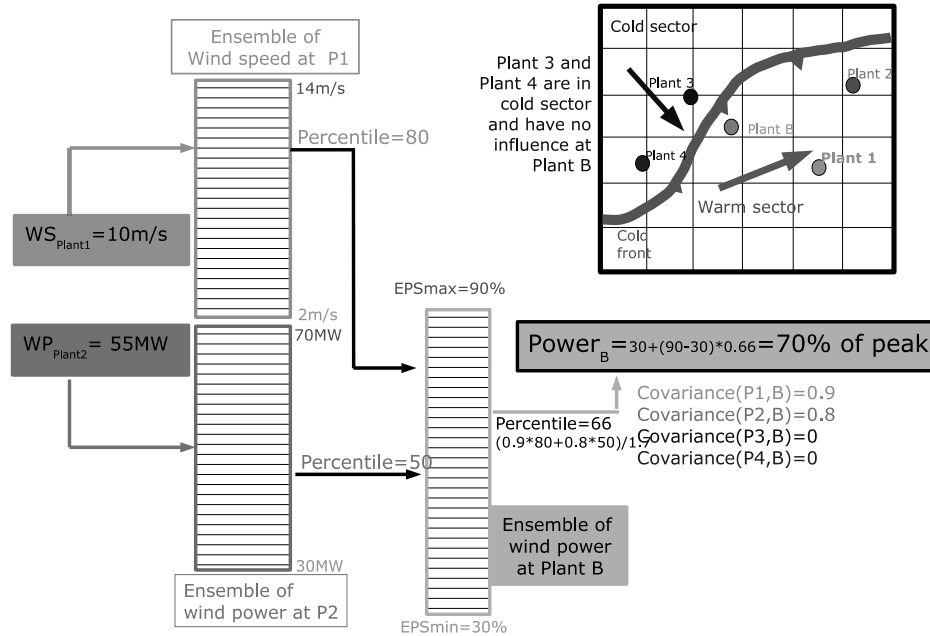


**Figure 7.** Functionality of the inverted Ensemble Kalman Filter when using different kind of measurements.

parameterisation schemes, 10 from the physical part of the model and 3 dynamical parameterisation schemes. Details of this system can be found in [30,114]. By applying physically possible outcomes from a 3-dimensional simulation of the atmosphere and transforming this into a vector in direct relation to the observation, a physically consistent data assimilation is possible. This approach is a major improvement and enhancement in energy meteorology as it opens the door to resolutions in time and space with minimal computational requirements for short-term or minute-scale forecasting, as the computational expensive work resides in the 6-hourly forecasting cycle of the ensemble. The assimilation of local measurements can be done on minute basis [28].

#### 5.5. Overview of methods for minute-scale forecasting

Table 2 provides an overview and summary of the different minute-scale prediction methods, their forecasting horizons as well as advantages and barriers to the adoption of the methods. It also lists solutions that are suggested as a way forward to overcome the barriers.

**Table 2.** Overview of methods for minute-scale forecasting

Type	Method	Input Data	Forecast Horizon	Advantage	Limitations	Next steps	References
Remote sensing based	Scanning lidar-based propagation models	Lidar data	1–30 min	<ul style="list-style-type: none"> <li>- Comprehensive knowledge of wind field several kilometres upstream</li> <li>- Scanning of vertical wind profiles for e.g. detection of low level jets</li> <li>- Compact size → flexible measurement campaigns, cost-competitive to met masts</li> </ul>	<ul style="list-style-type: none"> <li>- Fluctuating measurement range and forecast horizon due to environmental conditions</li> <li>- Ideal measurement setup for forecasting not clear, no standard available</li> <li>- Need for post processing is challenging in a real-time environment</li> </ul>	<ul style="list-style-type: none"> <li>- Need for a reliable fallback method if no data available</li> <li>- Investigation of different lidar cases to find best campaign setup → standards definition.</li> <li>- Regular service and calibration → ↓↓ risk of faulty signal processing but ↑ costs.</li> </ul>	[34,35,38,41]
	Radar-based density models	Doppler radar data	1–30min	<ul style="list-style-type: none"> <li>- Extended maximum measurement range (up to 35 km)</li> <li>- Reconstructed wind fields with high temporal (1-min) and spatial (50 m) resolution</li> <li>- Volumetric measurements allow to resolve information over the whole rotor area</li> </ul>	<ul style="list-style-type: none"> <li>- Data availability highly depends on the meteorological conditions</li> <li>- Large beam spread at large ranges → increased uncertainty</li> <li>- Large dimensions of the radar → complex installation</li> </ul>	<ul style="list-style-type: none"> <li>- Explore deeply and define the conditions and locations for optimal measurements</li> <li>- Investigate added value of installing a radar system for ramp event prediction in a wind farm cluster</li> </ul>	[56,57]
	Radar-based power fluctuations forecast	C and X-band weather radar data	10min–2h	<ul style="list-style-type: none"> <li>- Precipitation data highly correlates with strong fluctuations</li> <li>- Extended maximum measurement range → 60–240 km</li> <li>- Spatial resolution: 0.5–2 km / Temporal resolution: 1–15 minutes</li> </ul>	<ul style="list-style-type: none"> <li>- Clutter due to: wind turbine interference, meteorological targets</li> <li>- Measurement uncertainty increases with precipitation intensity</li> <li>- Underestimation of precipitation reflectivity during convective events</li> </ul>	<ul style="list-style-type: none"> <li>- Further development of pattern recognition techniques is required</li> <li>- Investigation on new wind turbine clutter detection and mitigation techniques</li> <li>- Improve cooperation between weather radars and wind energy communities</li> </ul>	[58,59]
Time Series Models	AR/ARMA models	Lidar, radar, sodar	15min–8h				–bah bah bah –bah bah bah
	Neural networks		15min–8h				
Data Assimilation methods	Lidar, radar, sodar, anemometers		15min–8h	<ul style="list-style-type: none"> <li>-These methods have a wide range of applicability and can incorporate different types of measurements</li> <li>-Extreme event analysis requires a diversity of observations</li> </ul>	<ul style="list-style-type: none"> <li>-Lack of use cases in power industry to prove the value of such information</li> <li>-Lack of standards and transparency of data exchange in power markets</li> </ul>	<ul style="list-style-type: none"> <li>- Setting up measurement campaigns with open data access for research and development</li> </ul>	[28,106]

## 750 6. Challenges for the implementation of minute-scale forecasting in large energy systems

751 There are several use cases for predictions shorter than 1 to 2 hours. In Australia, the system runs  
752 on a 5-min schedule [115] and requires renewable energy and load forecasts on those time scales. In  
753 Germany, renewable energy plants can be pre-qualified to participate in the reserve market, and need  
754 to predict their possible power with less than 5% accuracy in the pilot phase and less than 3.3% in  
755 the implementation phase. This is calculated in one-minute intervals. In Denmark, with hourly wind  
756 penetrations of over 140%, the grid is run proactively in hourly steps, predicting the imbalance and  
757 reacting accordingly on the basis of spatio-temporal forecasts [116]. So the use cases for minute scale  
758 forecasts are there, and the best forecasts require upstream information in real time.

759 In a large energy system with moderate penetration from wind sources, a system operator can  
760 choose to outsource balancing of wind. This is the approach chosen widely in central Europe. A major  
761 reason behind the liberalized strategy in Europe is a wish to make the market more competitive and  
762 indeed it happened faster than anybody expected in both Denmark (2009) and Germany (2012) [117]  
763 with the result of lower spot market prices in the NordPool market and the German-Austrian part of  
764 EPEX.

765 The difference between a TSO and a power trader's prioritized optimization lies in the target  
766 horizon. The trader is looking up to several weeks ahead, while the TSO's optimisation horizon is  
767 over one year. In particular once the commercial path is taken, then the TSO lacks information about  
768 the generation and must rely on the information from the trading companies. In Germany, the TSOs  
769 have today little control of the renewable energy generation and relies on out-sourced solutions for  
770 critical system information to a degree, which has not been considered acceptable for many years from  
771 a system security perspective.

772 Although Germany has the highest capacity of wind and solar generation in Europe, it is apparent  
773 that the system lacks information for optimization. This is seen in frequent down regulation of wind  
774 farms in day-time and recovery during the middle of the night, often many hours after the wind  
775 has dropped again. This process has become highly inefficient in recent years, because there are no  
776 requirements for wind farms to provide real-time data to the system operator.

777 German experience shows that wind energy loses efficiency and value unless there are obligations  
778 for wind farms to provide data required by various forecasting and system operation processes.

779 Based on this experience, it is crucial to define standards regarding setup and maintenance of  
780 instrumentation, collection and provision of data, as well as required quality of data. Beside the  
781 standards, in transparent markets the grid codes should also contain a clear definition about the rights  
782 on the use and the obligation to provide the data. Without such regulations, the required quality is  
783 hard to achieve in order to improve forecasts. Corrupt and wrongly calibrated instrumentation can do  
784 more damage to a forecast than not having data. This is one of the greatest challenges at present and  
785 the reason for slow progress on minute-scale forecasting. Especially in large systems such as Germany  
786 with many thousands of individual wind turbines and small wind farms, this is a difficult challenge to  
787 overcome. Nevertheless, the need to make appropriate changes to the grid codes is the same for all  
788 markets.

## 789 7. Conclusions

790 Minute-scale forecasting of wind power is a discipline that is becoming crucial to accomplish in  
791 globally transitioning power systems with increasing amounts of variable generating power sources  
792 from renewables. The participants of the collaborative IEA Wind Task 32 and 36 workshop established  
793 a framework for forecasting at the minute scale and discussed new techniques that will push the limits  
794 of state-of-the-art forecasting methods to a new level.

795 Three applications were identified that can benefit from minute-scale forecasting and their  
796 respective forecasting horizons. Wind turbine and wind farm controllers need wind speed forecasts  
797 to optimize the turbine and farm operation. The task of balancing the power grid and optimizing  
798 energy markets relies heavily on precise wind power forecasts as well. To carry out forecasts that range

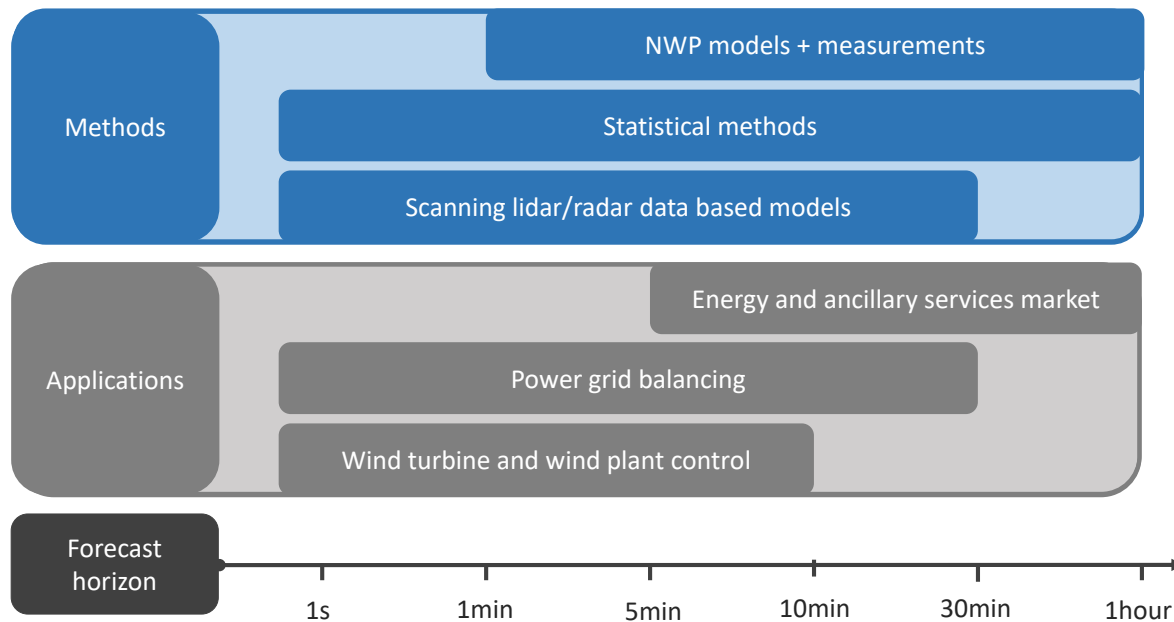


**Figure 8.** Overview of forecast horizons of different wind energy applications and forecast methods in the second and minute scale.

from 1 second to 60 minutes, forecasters have the choice between different methods (Figure 8). In our discussions at the workshop and this review we differentiate between using preview data from remote sensing devices, statistical approaches that deduce patterns from observational data to predict future values and finally methods that are based on data assimilation into physical models. These assimilated data can originate both from remote sensing devices or other existing observational data sources from meteorological masts or wind turbine data.

By investigating more deeply the respective methods it became clear that they all have advantages, but also barriers that need to be overcome in order to achieve reliable forecasts on a commercial level. The following list provides an overview of focus areas for the near future to advance further with minute-scale forecasting:

- **Research requirements.** At this point, many methods are still under development. There are a lot of open questions to solve and the optimal forecasting techniques for the different applications has not been found yet. It is also not sufficiently demonstrated that all methods add value. More research and especially more measurement campaigns using different types of instrumentation (lidars, radars, sodars and in situ measurements such as cup and sonic anemometers etc) to compare their benefits and disadvantages as individual signals but also as combinations of signals, needs to be carried out. Both measurement experts and meteorological modelers need to collaborate closely to find solutions.
- **Data requirements.** All forecasting methods rely on data. This might sound obvious, but what is needed is high resolution, high quality data delivered in real-time to forecast systems. Wind turbine or wind farm operators often only log 10-minute averages of their operational data. However, to train and validate models, high frequency data is necessary.
- **Requirement for standards.** End users have more confidence in data when the collection and use of the data is supported by recommended practices and standards. Community-driven recommended practices are available for some applications of wind lidar, but not in the context of forecasting.
- **Expert training.** As with any emerging technology, there are a limited number of experts that know how to carry out a remote sensing measurement campaign, feed data into neural networks

827 or are capable of assimilating data into a NWP model. This forms a barrier to the widespread  
828 commercialization of minutes-scale forecasting. IEA Wind Tasks provide an ideal platform for  
829 the international exchange and dissemination of knowledge order to establish more widespread  
830 training in this topic.

831 **Supplementary Materials:** IEA Wind Task 32 is operated by the Chair of Wind Energy at the Institute of Aircraft  
832 Design at the Faculty of Aerospace Engineering at the University of Stuttgart. More details about IEA Wind  
833 Task 32, including minutes from the workshops and other documents, can be found at [www.ieawindtask32.org](http://www.ieawindtask32.org). IEA Wind Task 36 Forecasting is operated by Gregor Giebel of DTU Wind Energy at Risø, Denmark.  
834 See [www.ieawindforecasting.dk](http://www.ieawindforecasting.dk) for more information. General information about IEA Wind can be found at  
835 [www.ieawind.org](http://www.ieawind.org). IEA Wind TCP functions within a framework created by the International Energy Agency.  
836 Views, findings, and publications of the IEA Wind TCP do not necessarily represent the views or policies of the  
837 IEA Secretariat or of all its individual member countries. IEA Wind TCP is part of IEA's Technology Collaboration  
838 Programme (TCP).

840 **Author Contributions:** Ines Würth was a co-organizer of the workshop, led the paper and wrote the abstract,  
841 introduction, Section 5.1.1, conclusion, some section introductions, and edited all sections. Laura Valldecabres  
842 Sanmartin was a co-organizer of the workshop, was a co-editor of this paper, led Section 2, 3.3 and 5.1.2 and  
843 contributed to Section 5.1.1, and 5.1. Elliot Simon was a co-organizer of the workshop, led Section 5.2, and  
844 contributed text in Sections: 2, 5.1.1, and 5.1. David Schlipf led Section 3.1. Bahri Uzunoglu led Section 3.2 and  
845 wrote Section 5.3 and 5.4 together with Corinna Mörlen who also led Section 4 and 5.1.4 and contributed to Section  
846 5.1, 5.2, 3.3 and 6. Gregor Giebel contributed to Section 4. Ciaran Gilbert contributed to Section 5.2. Anton Kaifel  
847 and all other co-authors participated in the paper review and revision process.

848 **Funding:** This publication was supported by the Open Access Publishing Fund of the University of Stuttgart and  
849 has received funding from the European Union's Horizon 2020 research and innovation programme under the  
850 Marie Skłodowska-Curie Grant No. 642108.

851 **Acknowledgments:** We would like to thank DTU Wind Energy (Risø campus) for graciously hosting the workshop,  
852 and all of the workshop participants who contributed their ideas and knowledge.

853 **Conflicts of Interest:** The authors declare no conflict of interest.

## 854 References

- 855 1. Giebel, G.; Brownsword, R.; Kariniotakis, G.; Denhard, M.; Draxl, C. The State-Of-The-Art in Short-Term  
856 Prediction of Wind Power. Technical report, Technical University of Denmark (DTU), Roskilde, Denmark,  
857 2011. doi:10.11581/DTU:00000017.
- 858 2. Fraile, D.; Mbistrova, A. Wind in power 2017: Annual combined onshore and offshore wind energy  
859 statistics. Technical report, WindEurope, 2018.
- 860 3. Fraile, D.; Komusanac, I. Wind energy in Europe: Outlook to 2022. Technical report, WindEurope, 2018.
- 861 4. Larsén, X.; Larsen, S.; Lundtang Petersen, E. Full-Scale Spectrum of Boundary-Layer Winds. *Boundary-Layer  
862 Meteorology* **2016**, *159*, 349–371. doi:10.1007/s10546-016-0129-x.
- 863 5. Apt, J. The spectrum of power from wind turbines. *Journal of Power Sources* **2007**, *169*, 369–374.  
864 doi:10.1016/j.jpowsour.2007.02.077.
- 865 6. Vincent, C.L.; Trombe, P.J. 8 - Forecasting intrahourly variability of wind generation. In *Renewable Energy  
866 Forecasting*; Kariniotakis, G., Ed.; Woodhead Publishing Series in Energy, Woodhead Publishing, 2017; pp.  
867 219 – 233. doi:<https://doi.org/10.1016/B978-0-08-100504-0.00008-1>.
- 868 7. Sørensen, P.; Cutululis, N.A.; Vigueras-Rodríguez, A.; Madsen, H.; Pinson, P.; Jensen, L.E.; Hjerrild, J.;  
869 Donovan, M. Modelling of power fluctuations from large offshore wind farms. *Wind Energy* **2008**, *11*, 29–43.  
870 doi:10.1002/we.246.
- 871 8. Akhmatov, V.; Abildgaard, H.; Pedersen, J.; Eriksen, P. Integration of Offshore Wind Power into the  
872 Western Danish Power System. *Proc. Copenhagen Offshore Wind 2005* **2005**.
- 873 9. van Kooten, G.C. Wind power: the economic impact of intermittency. *Letters in Spatial and Resource Sciences*  
874 **2010**, *3*, 1–17. doi:10.1007/s12076-009-0031-y.
- 875 10. Ela, E.; Kirby, B. ERCOT Event on February 26, 2008: Lessons Learned. Technical report, National  
876 Renewable Energy Laboratory, 2008. doi:10.2172/1218412.
- 877 11. Gallego-Castillo, C.; Cuerva-Tejero, A.; Lopez-Garcia, O. A review on the recent history of  
878 wind power ramp forecasting. *Renewable and Sustainable Energy Reviews* **2015**, *52*, 1148 – 1157.  
879 doi:10.1016/j.rser.2015.07.154.

- 880 12. Würth, I.; Ellinghaus, S.; Wigger, M.; Niemeier, M.J.; Clifton, A.; Cheng, P.W. Forecasting wind  
881 ramps: can long-range lidar increase accuracy? *Journal of Physics: Conference Series* **2018**, *1102*, 012013.  
882 doi:10.1088/1742-6596/1102/1/012013.
- 883 13. Schlipf, D.; Schlipf, D.J.; Kühn, M. Nonlinear model predictive control of wind turbines using LIDAR.  
884 *Wind Energy* **2013**, *16*, 1107–1129. doi:10.1002/we.1533.
- 885 14. Bossanyi, E. Combining induction control and wake steering for wind farm energy and fatigue loads  
886 optimisation. *J. Phys.: Conf. Ser.* **2018**, *1037*. doi:10.1088/1742-6596/1037/3/032011.
- 887 15. Momoh, J.A. *Smart grid: fundamentals of design and analysis*; Vol. 63, John Wiley & Sons, 2012.
- 888 16. Menin, M.; Uzunoglu, B. Parametric Sensitivity Study for Wind Power Trading through Stochastic Reserve  
889 and Energy Market Optimization. 2015 Seventh Annual IEEE Green Technologies Conference, 2015, pp.  
890 82–87. doi:10.1109/GREENTECH.2015.37.
- 891 17. Uzunoglu, B.; Bayazit, D. A generic resampling particle filter joint parameter estimation for electricity  
892 prices with jump diffusion. 2013 10th International Conference on the European Energy Market (EEM),  
893 2013, pp. 1–7. doi:10.1109/EEM.2013.6607409.
- 894 18. Uzunoglu, B.; AkifÜlker, M.; Bayazit, D. Particle filter joint state and parameter estimation of dynamic  
895 power systems. 2016 57th International Scientific Conference on Power and Electrical Engineering of Riga  
896 Technical University (RTUCON), 2016, pp. 1–7. doi:10.1109/RTUCON.2016.7763152.
- 897 19. Uzunoğlu, B.; Ülker, M.A. Maximum Likelihood Ensemble Filter State Estimation for Power Systems.  
898 *IEEE Transactions on Instrumentation and Measurement* **2018**, *67*, 2097–2106. doi:10.1109/TIM.2018.2814066.
- 899 20. Ülker, M.A.; Uzunoğlu, B. Simplex optimization for particle filter joint state and parameter estimation of  
900 dynamic power systems. *IEEE EUROCON 2017 -17th International Conference on Smart Technologies*,  
901 2017, pp. 399–404. doi:10.1109/EUROCON.2017.8011142.
- 902 21. Eriksson, R.; Modig, N.; Elkington, K. Synthetic inertia versus fast frequency response: a definition. *IET  
903 Renewable Power Generation* **2018**, *12*, 507–514. doi:10.1049/iet-rpg.2017.0370.
- 904 22. Díaz-González, F.; Haub, M.; Sumper, A.; Gomis-Bellmuntac, O. Participation of wind power plants  
905 in system frequency control: Review of grid code requirements and control methods. *Renewable and  
906 Sustainable Energy Reviews* **2014**, *43*, 551–564. doi:10.1016/j.rser.2014.03.040.
- 907 23. Mazzi, N.; Pinson, P. 10 - Wind power in electricity markets and the value of forecasting. In *Renewable  
908 Energy Forecasting*; Kariniotakis, G., Ed.; Woodhead Publishing Series in Energy, Woodhead Publishing,  
909 2017; pp. 259 – 278. doi:<https://doi.org/10.1016/B978-0-08-100504-0.00010-X>.
- 910 24. EPEX Spot SE. *Intraday Continous: Intraday Lead Times*, (accessed December 10, 2018).
- 911 25. NordPool. *Intraday Trading*, (accessed December 10, 2018).
- 912 26. Energy Exchange Istanbul (EXIST). *Intra-day Market*, (accessed December 10, 2018). <https://www.epias.com.tr/en/intra-day-market/phases>.
- 913 27. BSP South Pool. *Intraday Continous Market*, (accessed December 10, 2018). <https://www.bsp-southpool.com/intraday-continuous-market.html>.
- 914 28. Möhren, C., J.J. A new algorithm for Upscaling and Short-term forecasting of wind power using Ensemble  
915 forecasts; Energynautics GmbH: Bremen, Germany, 2009.
- 916 29. 50Hertz.; Amprion.; Tennet.; TransnetBW. Leitfaden zur Präqualifikation von Windenergieanlagen zur  
917 Erbringung von Minutenreserveleistung im Rahmen einer Pilotphase / Guidelines for Prequalification of  
918 Wind Turbines to provide Minute Reserves during a Pilot Phase. Technical report, German Transmission  
919 System Operators: Germany, German Transmission System Operators: Germany, 2016.
- 920 30. Pahlow, M.; Möhrlen, C.; Jørgensen, J., Application of cost functions for large-scale integration of wind  
921 power using a multi-scheme ensemble prediction technique; Optimization Advances in Electric Power  
922 Systems, NOVA Publisher NY, 2008.
- 923 31. IEC. Wind energy generation systems - Part 12-1: Power performance measurements of electricity  
924 producing wind turbines. Standard, International Electrotechnical Commission, Geneva, CH, 2017.
- 925 32. Clifton, A.; Clive, P.; Gottschall, J.; Schlipf, D.; Simley, E.; Simmons, L.; Stein, D.; Trabucchi, D.; Vasiljevic,  
926 N.; Würth, I. IEA Wind Task 32: Wind Lidar - Identifying and mitigating barriers to the adoption of wind  
927 lidar. *Remote Sensing* **2018**, *10*, 413–433. doi:10.3390/rs10030406.
- 928 33. Emeis, S.; Harris, M.; Banta, R.M. Boundary-layer anemometry by optical remote sensing for wind energy  
929 applications. *Meteorologische Zeitschrift* **2007**, *16*, 337–347. doi:10.1127/0941-2948/2007/0225.
- 930

- 932 34. Simley, E.; Pao, L.Y.; Frehlich, R.; Jonkman, B.; Kelley, N. Analysis of light detection and ranging wind  
933 speed measurements for wind turbine control. *Wind Energy* **2014**, *17*, 413–433. doi:10.1002/we.1584.
- 934 35. Clifton, A.; Boquet, M.; Burin Des Roziers, E.; Westerhellweg, A.; Hofsass, M.; Klaas, T.; Vogstad, K.; Clive,  
935 P.; Harris, M.; Wylie, S.; Osler, E.; Banta, B.; Choukulkar, A.; Lundquist, J.; Aitken, M. Remote Sensing  
936 of Complex Flows by Doppler Wind Lidar: Issues and Preliminary Recommendations. Technical Report  
937 TP-5000-64634, National Renewable Energy Laboratory, 2015.
- 938 36. Vasiljević, N.; L. M. Palma, J.M.; Angelou, N.; Carlos Matos, J.; Menke, R.; Lea, G.; Mann, J.; Courtney, M.;  
939 Frölen Ribeiro, L.; M. G. C. Gomes, V.M. Perdigão 2015: methodology for atmospheric multi-Doppler lidar  
940 experiments. *Atmospheric Measurement Techniques* **2017**, *10*, 3463–3483. doi:10.5194/amt-10-3463-2017.
- 941 37. Courtney, M.; Simon, E. *Deploying scanning lidars at coastal sites*; DTU Wind Energy: Denmark, 2016.
- 942 38. Valldécabres, L.; Peña, A.; Courtney, M.; von Bremen, L.; Kühn, M. Very short-term forecast of near-coastal  
943 flow using scanning lidars. *Wind Energy Science* **2018**, *3*, 313–327. doi:10.5194/wes-3-313-2018.
- 944 39. Simon, E.; Courtney, M.; Vasiljevic, N. Minute-Scale Wind Speed Forecasting Using Scanning Lidar Inflow  
945 Measurements. *Wind Energy Science Discussions* **2018**. doi:10.5194/wes-2018-71.
- 946 40. Kokhanovsky, A. *Aerosol Optics: Light Absorption and Scattering by Particles in the Atmosphere*; Springer-Verlag  
947 Berlin Heidelberg, 2008.
- 948 41. Würth, I.; Brenner, A.; Wigger, M.; Cheng, P.W. How far do we see? Analysis of the measurement range of  
949 long-range lidar data for wind power forecasting. German Wind Energy Conference DEWEK, 2017.
- 950 42. Performance Verification of Galion. Technical Report Report 13001, Deutsche Windguard, 2013.
- 951 43. Bradley, S. Wind speed errors for LIDARs and SODARs in complex terrain. *IOP Conference Series: Earth  
952 and Environmental Science* **2008**, *1*, 012061.
- 953 44. Bradley, S.; Perrott, Y.; Behrens, P.; Oldroyd, A. Corrections for wind-speed errors from Sodar and Lidar in  
954 complex terrain. *Boundary-Layer Meteorology* **2012**, *143*, 37–48. doi:10.1007/s10546-012-9702-0.
- 955 45. Bradley, S.; von Hünerbein, S.; Mikkelsen, T. A bistatic Sodar for precision wind profiling in complex  
956 terrain. *Journal of Atmospheric and Oceanic Technology* **2012**, *29*, 1052–1061. doi:10.1175/JTECH-D-11-00035.1.
- 957 46. Emeis, S.; Harris, M.; Banta, R.M. Boundary-layer anemometry by optical remote sensing for wind energy  
958 applications. *Meteorologische Zeitschrift* **2007**, *16*, 337–347. doi:10.1127/0941-2948/2007/0225.
- 959 47. Kindler, D.; Oldroyd, A.; MacAskill, A.; Finch, D. An eight month test campaign of the Qinetiq ZephIR  
960 system: Preliminary results. *Meteorologische Zeitschrift* **2007**, *16*, 479–489. doi:10.1127/0941-2948/2007/0226.
- 961 48. Yang, Q.; Berg, L.; Pekour, M.; Fast, J.; Newsom, R. Evaluation of WRF-Predicted Near-Hub-Height Winds  
962 and Ramp Events over a Pacific Northwest Site with Complex Terrain. *J. of Appl. Meteo. and Climatology*  
963 **2013**, *52*, 1753–1763. doi:10.1175/JAMC-D-12-0267.1.
- 964 49. Clifton, A.; M.Boquet.; Burin, E.; Hofst  , M.; Klaas, T.; Vogstad, K.; Clive, P.; Harris, M.; Wylie, S.; E.Osler.;  
965 Banta, R.; Choukulkar, A.; Lundquist, J.; Aitken., M. Remote Sensing of Complex Flows by Doppler  
966 Wind Lidar: Issues and Preliminary Recommendations. Technical report, National Renewable Energy  
967 Laboratory, 15013 Denver West Parkway, Golden, CO 80401, 2015.
- 968 50. Vasiljević, N.; L. M. Palma, J.M.; Angelou, N.; Carlos Matos, J.; Menke, R.; Lea, G.; Mann, J.; Courtney, M.;  
969 Fr  len Ribeiro, L.; M. G. C. Gomes, V.M. Perdig  o 2015: methodology for atmospheric multi-Doppler lidar  
970 experiments. *Atmospheric Measurement Techniques* **2017**, *10*, 3463–3483. doi:10.5194/amt-10-3463-2017.
- 971 51. Wulfmeyer, V.; Turner, D.D.; Baker, B.; Banta, R.; Behrendt, A.; Bonin, T.; Brewer, W.A.; Buban, M.;  
972 Choukulkar, A.; Dumas, E.; Hardesty, R.M.; Heus, T.; Ingwersen, J.; Lange, D.; Lee, T.R.;  
973 Metzendorf, S.; Muppa, S.K.; Meyers, T.; Newsom, R.; Osman, M.; Raasch, S.; Santanello, J.; Senff, C.;  
974 Sp  th, F.; Wagner, T.; Weckwerth, T. A New Research Approach for Observing and Characterizing  
975 Land-Atmosphere Feedback. *Bulletin of the American Meteorological Society* **2018**, *99*, 1639–1667,  
976 [<https://doi.org/10.1175/BAMS-D-17-0009.1>]. doi:10.1175/BAMS-D-17-0009.1.
- 977 52. Hirth, B.D.; Schroeder, J.L.; Gunter, W.S.; Guynes, J.G. Measuring a Utility-Scale Turbine Wake Using  
978 the TTUKa Mobile Research Radars. *Journal of Atmospheric and Oceanic Technology* **2012**, *29*, 765–771.  
979 doi:10.1175/JTECH-D-12-00039.1.
- 980 53. Hirth, B.D.; Schroeder, J.L.; Gunter, W.S.; Guynes, J.G. Coupling Doppler radar-derived wind maps  
981 with operational turbine data to document wind farm complex flows. *Wind Energy* **2015**, *18*, 529–540.  
982 doi:10.1002/we.1701.
- 983 54. Nygaard, N.G.; Newcombe, A.C. Wake behind an offshore wind farm observed with dual-Doppler radars.  
984 *Journal of Physics: Conference Series* **2018**, *1037*, 072008. doi:10.1088/1742-6596/1037/7/072008.

- 985 55. Marathe, N.; Swift, A.; Hirth, B.; Walker, R.; Schroeder, J. Characterizing power performance and wake of  
986 a wind turbine under yaw and blade pitch. *Wind Energy* **2016**, *19*, 963–978. doi:10.1002/we.1875.
- 987 56. Hirth, B.D.; Schroeder, J.L.; Irons, Z.; Walter, K. Dual-Doppler measurements of a wind ramp event at an  
988 Oklahoma wind plant. *Wind Energy* **2016**, *19*, 953–962. doi:10.1002/we.1867.
- 989 57. Valldecabres, L.; Nygaard, N.G.; Vera-Tudela, L.; von Bremen, L.; Kühn, M. On the Use of  
990 Dual-Doppler Radar Measurements for Very Short-Term Wind Power Forecasts. *Remote Sensing* **2018**, *10*.  
991 doi:10.3390/rs10111701.
- 992 58. Trombe, P.J.; Pinson, P.; Vincent, C.; Bøvith, T.; Cutululis, N.A.; Draxl, C.; Giebel, G.; N.Hahmann, A.;  
993 E.Jensen, N.; Jensen, B.P.; Le, N.F.; Madsen, H.; Pedersen, L.B.; Sommer, A. Weather radars – the new eyes  
994 for offshore wind farms? *Wind Energy* **2014**, *17*, 1767–1787. doi:10.1002/we.1659.
- 995 59. Trombe, P.; Pinson, P.; Madsen, H. Automatic Classification of Offshore Wind Regimes With Weather  
996 Radar Observations. *IEEE Journal of Selected Topics in Applied Earth Observations and Remote Sensing* **2014**,  
997 *7*, 116–125. doi:10.1109/JSTARS.2013.2252604.
- 998 60. Freedman, J.M.; Manobianco, J.; Schroeder, J.; Ancell, B.; Brewster, K.; Basu, S.; Banunarayanan, V.;  
999 Hodge, B.M.; Flores, I. The Wind Forecast Improvement Project (WFIP): A Public/Private Partnership for  
1000 Improving Short Term Wind Energy Forecasts and Quantifying the Benefits of Utility Operations. The  
1001 Southern Study Area, Final Report **2014**. doi:10.2172/1129905.
- 1002 61. *Meteorological Assimilation Data Ingest System (MADIS)*, (accessed December 10, 2018).
- 1003 62. Wilczak, J.; Finley, C.; Freedman, J.; Cline, J.; Bianco, L.; Olson, J.; Djalalova, I.; Sheridan, L.; Ahlstrom,  
1004 M.; Manobianco, J.; Zack, J.; Carley, J.R.; Benjamin, S.; Coulter, R.; Berg, L.K.; Mirocha, J.; Clawson, K.;  
1005 Naterberg, E.; Marquis, M. The Wind Forecast Improvement Project (WFIP): A Public–Private Partnership  
1006 Addressing Wind Energy Forecast Needs. *Bull. Amer. Meteor. Soc.* **2015**, *96*, 1699–1718.
- 1007 63. Nakafuji, D. Distributed Resource Energy Analysis & Management System (DREAMS) Development for  
1008 Real-time Grid Operations. Technical Report DOE-EE0006331-FTR1, Hawaiian Electric Company to U.S.  
1009 Department of Energy, 2016.
- 1010 64. Pinson, P. Very-short-term probabilistic forecasting of wind power with generalized logit–normal  
1011 distributions. *Journal of the Royal Statistical Society: Series C (Applied Statistics)* **2012**, *61*, 555–576.  
1012 doi:10.1111/j.1467-9876.2011.01026.x.
- 1013 65. Torres, J.; García, A.; Blas, M.D.; Francisco, A.D. Forecast of hourly average wind speed with ARMA models  
1014 in Navarre (Spain). *Solar Energy* **2005**, *79*, 65 – 77. doi:<https://doi.org/10.1016/j.solener.2004.09.013>.
- 1015 66. Erdem, E.; Shi, J. ARMA based approaches for forecasting the tuple of wind speed and direction. *Applied  
1016 Energy* **2011**, *88*, 1405 – 1414. doi:<https://doi.org/10.1016/j.apenergy.2010.10.031>.
- 1017 67. Li, G.; Shi, J. On comparing three artificial neural networks for wind speed forecasting. *Applied Energy*  
1018 **2010**, *87*, 2313 – 2320. doi:<https://doi.org/10.1016/j.apenergy.2009.12.013>.
- 1019 68. Feng, C.; Cui, M.; Hodge, B.M.; Zhang, J. A data-driven multi-model methodology with  
1020 deep feature selection for short-term wind forecasting. *Applied Energy* **2017**, *190*, 1245 – 1257.  
1021 doi:<https://doi.org/10.1016/j.apenergy.2017.01.043>.
- 1022 69. Niu, T.; Wang, J.; Zhang, K.; Du, P. Multi-step-ahead wind speed forecasting based on optimal feature  
1023 selection and a modified bat algorithm with the cognition strategy. *Renewable Energy* **2018**, *118*, 213–229.  
1024 doi:10.1016/j.renene.2017.10.075.
- 1025 70. Pinson, P. Introducing distributed learning approaches in wind power forecasting. 2016  
1026 International Conference on Probabilistic Methods Applied to Power Systems (PMAPS), 2016, pp. 1–6.  
1027 doi:10.1109/PMAPS.2016.7764224.
- 1028 71. Hochreiter, S.; Schmidhuber, J. Long Short-Term Memory. *Neural Computation* **1997**, *9*, 1735–1780.  
1029 doi:10.1162/neco.1997.9.8.1735.
- 1030 72. Wu, W.; Chen, K.; Qiao, Y.; Lu, Z. Probabilistic short-term wind power forecasting based on deep neural  
1031 networks. 2016 International Conference on Probabilistic Methods Applied to Power Systems (PMAPS),  
1032 2016, pp. 1–8. doi:10.1109/PMAPS.2016.7764155.
- 1033 73. Ailliot, P.; Monbet, V. Markov-switching autoregressive models for wind time series. *Environmental  
1034 Modelling & Software* **2012**, *30*, 92 – 101. doi:<https://doi.org/10.1016/j.envsoft.2011.10.011>.
- 1035 74. Pinson, P.; Madsen, H. Adaptive modelling and forecasting of offshore wind power fluctuations with  
1036 Markov-switching autoregressive models. *Journal of Forecasting* **2012**, *31*, 281–313. doi:10.1002/for.1194.

- 1037 75. Browell, J.; Drew, D.R.; Philippopoulos, K. Improved very short-term spatio-temporal wind forecasting  
1038 using atmospheric regimes. *Wind Energy* **2018**, *0*. doi:10.1002/we.2207.
- 1039 76. Browell, J.; Gilbert, C. Cluster-based regime-switching AR for the EEM 2017 Wind Power Forecasting  
1040 Competition. 2017 14th International Conference on the European Energy Market (EEM), 2017, pp. 1–6.  
1041 doi:10.1109/EEM.2017.7982034.
- 1042 77. Hering, A.S.; Genton, M.G. Powering Up With Space-Time Wind Forecasting. *Journal of the American  
1043 Statistical Association* **2010**, *105*, 92–104. doi:10.1198/jasa.2009.ap08117.
- 1044 78. Dowell, J.; Pinson, P. Very-Short-Term Probabilistic Wind Power Forecasts by Sparse Vector Autoregression.  
1045 *IEEE Transactions on Smart Grid* **2016**, *7*, 763–770. doi:10.1109/TSG.2015.2424078.
- 1046 79. Messner, J.W.; Pinson, P. Online adaptive lasso estimation in vector autoregressive models  
1047 for high dimensional wind power forecasting. *International Journal of Forecasting* **2018**.  
1048 doi:<https://doi.org/10.1016/j.ijforecast.2018.02.001>.
- 1049 80. Cavalcante, L.; Bessa, R.J.; Reis, M.; Browell, J. LASSO vector autoregression structures for very short-term  
1050 wind power forecasting. *Wind Energy* **2017**, *20*, 657–675. doi:10.1002/we.2029.
- 1051 81. Zhang, Y.; Wang, J.; Wang, X. Review on probabilistic forecasting of wind power generation. *Renewable and  
1052 Sustainable Energy Reviews* **2014**, *32*, 255–270. doi:10.1016/j.rser.2014.01.033.
- 1053 82. Dowell, J.; Pinson, P. Very-Short-Term Probabilistic Wind Power Forecasts by Sparse Vector Autoregression.  
1054 *IEEE Transactions on Smart Grid* **2016**, *7*, 763–770. doi:10.1109/TSG.2015.2424078.
- 1055 83. Jeon, J.; Taylor, J.W. Using Conditional Kernel Density Estimation for Wind Power Density Forecasting.  
1056 *Journal of the American Statistical Association* **2012**, *107*, 66–79. doi:10.1080/01621459.2011.643745.
- 1057 84. Wan, C.; Xu, Z.; Pinson, P.; Dong, Z.Y.; Wong, K.P. Probabilistic Forecasting of Wind Power  
1058 Generation Using Extreme Learning Machine. *IEEE Transactions on Power Systems* **2014**, *29*, 1033–1044.  
1059 doi:10.1109/TPWRS.2013.2287871.
- 1060 85. Bessa, R.J.; Möhrlein, C.; Fundel, V.; Siefert, M.; Browell, J.; Haglund El Gaidi, S.; Hodge, B.M.; Cali, U.;  
1061 Kariniotakis, G. Towards Improved Understanding of the Applicability of Uncertainty Forecasts in the  
1062 Electric Power Industry. *Energies* **2017**, *10*. doi:10.3390/en10091402.
- 1063 86. Yıldırım, N.; Uzunoğlu, B., Data Mining via Association Rules for Power Ramps Detected by Clustering or  
1064 Optimization. In *Transactions on Computational Science XXVIII: Special Issue on Cyberworlds and Cybersecurity*;  
1065 Springer Berlin Heidelberg: Berlin, Heidelberg, 2016; pp. 163–176. doi:10.1007/978-3-662-53090-0\_9.
- 1066 87. Yıldırım, N.; Uzunoğlu, B. Spatial Clustering for Temporal Power Ramp Balance and Wind Power  
1067 Estimation. 2015 Seventh Annual IEEE Green Technologies Conference, 2015, pp. 214–220.  
1068 doi:10.1109/GREENTECH.2015.39.
- 1069 88. Yıldırım, N.; Uzunoğlu, B. Association Rules for Clustering Algorithms for Data Mining of Temporal  
1070 Power Ramp Balance. 2015 International Conference on Cyberworlds (CW), 2015, pp. 224–228.  
1071 doi:10.1109/CW.2015.72.
- 1072 89. Dey, C. Evolution of objective analysis methods of NMC's Medium-Range Model. *Wea. Forecasting* **1989**,  
1073 *4*, 391–400.
- 1074 90. Ide, K.; Courtier, P.; Ghil, M.; Lorenc, A.C. Unified Notation for Data Assimilation: Operational, Sequential  
1075 and Variational. *Journal of the Meteorological Society of Japan. Ser. II, Special Issue on Data Assimilation in  
1076 Meteorology and Oceanography: Theory and practice* **1997**, *75*, 181–189. doi:10.2151/jmsj1965.75.1B\_181.
- 1077 91. Cressman, G.P. An operational objective analysis system. *Monthly Weather Review* **1959**, *87*, 367–374.  
1078 doi:10.1175/1520-0493(1959)087<0367:AOOAS>2.0.CO;2.
- 1079 92. Gandin, L., Objective Analysis of meteorological fields; Gidromet, English translation Jerusalem: Israel  
1080 program for scientific translation, 1965.
- 1081 93. Kanamitsu, M. Description of the NMC Global Data Assimilation and Forecast System. *Weather and  
1082 Forecasting* **1989**, *4*, 335–342. doi:10.1175/1520-0434(1989)004<0335:DOTNGD>2.0.CO;2.
- 1083 94. Courtier, P.; Andersson, E.; Heckley, W.; Vasiljevic, D.; Hamrud, M.; Hollingsworth, A.; Rabier, F.;  
1084 Fisher, M.; Pailleux, J. The ECMWF implementation of three-dimensional variational assimilation  
1085 (3D-Var). I: Formulation. *Quarterly Journal of the Royal Meteorological Society* **1998**, *124*, 1783–1807.  
1086 doi:10.1002/qj.49712455002.
- 1087 95. Wu, W.S.; Purser, R.J.; Parrish, D.F. Three-Dimensional Variational Analysis with  
1088 Spatially Inhomogeneous Covariances. *Monthly Weather Review* **2002**, *130*, 2905–2916.  
1089 doi:10.1175/1520-0493(2002)130<2905:TDVAWS>2.0.CO;2.

- 1090 96. Courtier, P.; Thépaut, J.N.; Hollingsworth, A. A strategy for operational implementation of 4D-Var,  
1091 using an incremental approach. *Quarterly Journal of the Royal Meteorological Society* **1994**, *120*, 1367–1387.  
1092 doi:10.1002/qj.49712051912.
- 1093 97. Zupanski, D. A General Weak Constraint Applicable to Operational 4DVAR Data Assimilation Systems.  
1094 *Monthly Weather Review* **1997**, *125*, 2274–2292. doi:10.1175/1520-0493(1997)125<2274:AGWCAT>2.0.CO;2.
- 1095 98. Evensen, G. Sequential data assimilation with a nonlinear quasi-geostrophic model using Monte Carlo  
1096 methods to forecast error statistics. *Journal of Geophysical Research: Oceans* **1994**, *99*, 10143–10162,  
1097 [<https://agupubs.onlinelibrary.wiley.com/doi/pdf/10.1029/94JC00572>]. doi:10.1029/94JC00572.
- 1098 99. Turner, M.; Walker, J.; Oke, P. Ensemble member generation for sequential data assimilation. *Remote  
1099 Sensing of Environment* **2008**, *112*, 1421 – 1433. Remote Sensing Data Assimilation Special Issue,  
1100 doi:<https://doi.org/10.1016/j.rse.2007.02.042>.
- 1101 100. Kalman, R.; Bucy, R.S. New Results in Linear Filtering and Prediction Theory. *ASME. J. Basic Eng.* **1961**,  
1102 *83*, 95–108. doi:10.1115/1.3658902.
- 1103 101. Jazwinski, A. *Stochastic Processes and Filtering Theory*; Mathematics in Science and Engineering, Elsevier  
1104 Science, 1970.
- 1105 102. Ristic, B.; Arulampalm, S.; Gordon, N. *Beyond the Kalman filter: particle filters for tracking applications*; The  
1106 Artech House radar library, Artech House, Incorporated, 2004.
- 1107 103. Todling, R.; Cohn, S.E.; Sivakumaran, N.S. Suboptimal Schemes for Retrospective Data Assimilation  
1108 Based on the Fixed-Lag Kalman Smoother. *Monthly Weather Review* **1998**, *126*, 2274–2286.  
1109 doi:10.1175/1520-0493(1998)126<2274:SSFRDA>2.0.CO;2.
- 1110 104. Anderson, J.L. An Ensemble Adjustment Kalman Filter for Data Assimilation. *Monthly Weather Review*  
1111 **2001**, *129*, 2884–2903. doi:10.1175/1520-0493(2001)129<2884:AEAKFF>2.0.CO;2.
- 1112 105. Houtekamer, P.L.; Mitchell, H.L. A Sequential Ensemble Kalman Filter for Atmospheric Data Assimilation.  
1113 *Monthly Weather Review* **2001**, *129*, 123–137. doi:10.1175/1520-0493(2001)129<0123:ASEKFF>2.0.CO;2.
- 1114 106. Meng, Z.; Zhang, F. Tests of an Ensemble Kalman Filter for Mesoscale and Regional-Scale Data  
1115 Assimilation. Part II: Imperfect Model Experiments. *Monthly Weather Review* **2007**, *135*, 1403–1423.  
1116 doi:10.1175/MWR3352.1.
- 1117 107. Xiong, X.; Navon, I.M.; Uzunoglu, B. A Note on the Particle Filter with Posterior Gaussian Resampling.  
1118 *Tellus A: Dynamic Meteorology and Oceanography* **2006**, *58*, 456–460. doi:10.1111/j.1600-0870.2006.00185.x.
- 1119 108. Uzunoglu, B.; Fletcher, S.J.; Zupanski, M.; Navon, I.M. Adaptive ensemble reduction and inflation.  
1120 *Quarterly Journal of the Royal Meteorological Society* **2007**, *133*, 1281–1294. doi:10.1002/qj.96.
- 1121 109. Zupanski, M. Maximum Likelihood Ensemble Filter: Theoretical Aspects. *Monthly Weather Review* **2005**,  
1122 *133*, 1710–1726. doi:10.1175/MWR2946.1.
- 1123 110. Houtekamer, P.L.; Mitchell, H.L.; Pellerin, G.; Buehner, M.; Charron, M.; Spacek, L.; Hansen, B. Atmospheric  
1124 Data Assimilation with an Ensemble Kalman Filter: Results with Real Observations. *Monthly Weather  
1125 Review* **2005**, *133*, 604–620. doi:10.1175/MWR-2864.1.
- 1126 111. Hamill, T.M.; Snyder, C. Using Improved Background-Error Covariances from an Ensemble  
1127 Kalman Filter for Adaptive Observations. *Monthly Weather Review* **2002**, *130*, 1552–1572.  
1128 doi:10.1175/1520-0493(2002)130<1552:UIBECF>2.0.CO;2.
- 1129 112. Snyder, C.; Zhang, F. Assimilation of Simulated Doppler Radar Observations with an Ensemble Kalman  
1130 Filter. *Monthly Weather Review* **2003**, *131*, 1663–1677. doi:10.1175//2555.1.
- 1131 113. Zhang, F.; Snyder, C.; Sun, J. Impacts of Initial Estimate and Observation Availability on Convective-Scale  
1132 Data Assimilation with an Ensemble Kalman Filter. *Monthly Weather Review* **2004**, *132*, 1238–1253.  
1133 doi:10.1175/1520-0493(2004)132<1238:IOIEAO>2.0.CO;2.
- 1134 114. Möhrlen, C. Uncertainty in wind energy forecasting. PhD thesis, National University of Ireland, Cork,  
1135 Ireland, 2004.
- 1136 115. DISPATCH. Technical report, Australiaen Electricity Market Operator (AEMO), Level 22, 530 Collins Street  
1137 Melbourne VIC 3000, Australia, 2018.
- 1138 116. Borup, L. IEA Wind Task 36 Forecasting webinar: How to run 40% RE in the Danish system.  
1139 <https://www.youtube.com/watch?v=IGhUasWctUM>, last accessed 3. 12. 2018, 2018.
- 1140 117. Germany, B. *EEG in Zahlen* 2016, 2016.

<sup>1141</sup> © 2019 by the authors. Submitted to *Energies* for possible open access publication under the terms and conditions  
<sup>1142</sup> of the Creative Commons Attribution (CC BY) license (<http://creativecommons.org/licenses/by/4.0/>).